Available online at www.sciencedirect.com
SCIENCE DIRECT®

Global and Planetary Change 52 (2006) 142 – 172

GLOBAL AND PLANETARY CHANGE

www.elsevier.com/locate/gloplacha

Aeolian dust experiment on climate impact: An overview of Japan–China joint project ADEC

M. Mikami [a,*], G.Y. Shi [b], I. Uno [c], S. Yabuki [d], Y. Iwasaka [e], M. Yasui [f], T. Aoki [a], T.Y. Tanaka [a], Y. Kurosaki [g], K. Masuda [a], A. Uchiyama [a], A. Matsuki [h], T. Sakai [h], T. Takemi [i], M. Nakawo [j], N. Seino [a], M. Ishizuka [k], S. Satake [j], K. Fujita [h], Y. Hara [l], K. Kai [h], S. Kanayama [d], M. Hayashi [m], M. Du [n], Y. Kanai [o], Y. Yamada [d], X.Y. Zhang [p], Z. Shen [q], H. Zhou [r], O. Abe [s], T. Nagai [a], Y. Tsutsumi [t], M. Chiba [a], J. Suzuki [u]

[a] *Meteorological Research Institute, Nagamine 1-1, Tsukuba, Ibaraki 305-0052, Japan*
[b] *Institute of Atmospheric Physics, CAS, Deshengmenwai Qijiahuozi, Beijing 100029, China*
[c] *Research Institute for Applied Mechanics, Kyusyu University, Kasuga, Fukuoka 816-8580, Japan*
[d] *RIKEN, Wako-shi, Saitama 351-0198, Japan*
[e] *Institute of Nature and Environmental Technology, Kanazawa University, Kanazawa, Ishikawa 920-1192, Japan*
[f] *Communications Research Laboratory, Koganei, Tokyo 184-0015, Japan*
[g] *Center for Environmental Remote Sensing, Chiba University, Inage, Chiba 263-8522, Japan*
[h] *Graduate School of Environmental Studies, Nagoya University, Chikusa-ku, Nagoya 464-8601, Japan*
[i] *Department of Environmental Science and Technology, Tokyo Institute of Technology, Yokohama, Kanagawa 226-8502, Japan*
[j] *Research Institute for Humanity and Nature, Kamigyo-ku, Kyoto 602-0878, Japan*
[k] *Faculty of Engineering, Kagawa University, Takamatsu, Kagawa 761-0396, Japan*
[l] *Earth System Science and Technology, Kyusyu University, Kasuga, Fukuoka 816-8580, Japan*
[m] *Graduate School of Science, Fukuoka University, Jonan-ku, Fukuoka 814-0180, Japan*
[n] *National Institute for Agro-Environmental Sciences, Tsukuba, Ibaraki 305-8604, Japan*
[o] *Geological Survey of Japan, National Institute of Advanced Industrial Science and Technology, Tsukuba, Ibaraki 305-8567, Japan*
[p] *Chinese Academy of Meteorological Sciences, Zhong-Guan-Cun South Avenue, Beijing 100081, China*
[q] *Cold and Arid Regions Environmental and Engineering Research Institute, CAS, 316 Donggang West Road, Lanzhou 730000, China*
[r] *Xinjiang Institute of Ecology and Geography, CAS, 40-3, South Beijing Road, Urumqi, Xinjiang 830011, China*
[s] *National Research Institute for Earth Science and Disaster Prevention, Shinjo, Yamagata 996-0091, Japan*
[t] *Japan Meteorological Agency, Chiyoda-ku, Tokyo 100-8122, Japan*
[u] *METOCEAN Environment Inc., Setagaya-ku, Tokyo 154-8585, Japan*

Available online 2 May 2006

Abstract

The Aeolian Dust Experiment on Climate Impact (ADEC) was initiated in April 2000 as a joint five-year Japan–China project. The goal was to understand the impact of aeolian dust on climate via radiative forcing (RF). Field experiments and numerical simulations were conducted from the source regions in northwestern China to the downwind region in Japan in order to understand wind erosion processes temporal and spatial distribution of dust during their long-range transportation chemical, physical, and optical properties of dust and the direct effect of radiative forcing due to dust. For this, three intensive observation periods (IOP) were conducted from April 2002 to April 2004.

* Corresponding author. Tel.: +81 29 853 8623; fax: +81 29 855 7240.
E-mail address: mmikami@mri-jma.go.jp (M. Mikami).

doi:10.1016/j.gloplacha.2006.03.001

The in situ and network observation results are summarized as follows: (1) In situ observations of the wind erosion process revealed that the vertical profile of moving sand has a clear size dependency with height and saltation flux and that threshold wind velocity is dependent on soil moisture. Results also demonstrated that saltation flux is strongly dependent on the parent soil size distribution of the desert surface. (2) Both lidar observations and model simulations revealed a multiple dust layer in East Asia. A numerical simulation of a chemical transport model, CFORS, illustrated the elevated dust layer from the Taklimakan Desert and the lower dust layer from the Gobi Desert. The global-scale dust model, MASINGAR, also simulated the dust layer in the middle to upper free troposphere in East Asia, which originated from North Africa and the Middle East during a dust storm in March 2003. Raman lidar observations at Tsukuba, Japan, found the ice cloud associated with the dust layer at an altitude of 6 to 9 km. Analysis from lidar and the radio-sonde observation suggested that the Asian dust acted as ice nuclei at the ice-saturated region. These results suggest the importance of dust's climate impact via the indirect effect of radiative forcing due to the activation of dust into ice nuclei. (3) Studies on the aerosol concentration indicated that size distributions of aerosols in downwind regions have bimodal peaks. One peak was in the submicron range and the other in the supermicron range. The main soluble components of the supermicron peak were Na^+, Ca^{2+}, NO_3^-, and Cl^-. In the downwind region in Japan, the dust, sea salt, and a mixture of the two were found to be dominant in coarse particles in the mixed boundary layer. (4) Observation of the optical properties of dust by sky-radiometer, particle shoot absorption photometer (PSAP), and Nephelometer indicated that unpolluted dust at source region has a weaker absorption than originally believed.

A sensitivity experiment of direct RF by dust indicated that single scattering albedo is the most important of the optical properties of dust and that the sensitivity of instantaneous RF in the shortwave region at the top of the atmosphere to the refractive index strongly depends on surface albedo. A global scale dust model, MASINGAR, was used for evaluation of direct RF due to dust. The results indicated the global mean RF at the top and the bottom of the atmosphere were −0.46 and −2.13 W m^{-2} with cloud and were almost half of the RF with cloud-free condition.

Keywords: aerosol; aeolian dust; Asian dust; climate; wind erosion; radiative forcing

1. Introduction

Aeolian dust drifting from arid and semi-arid regions of the continents causes serious damage to the local ecosystem and human society in those regions. It is also an important factor in the global climate system (Fig. 1). Aeolian dust particles in the atmosphere play an important role in the radiative forcing (RF) of the atmosphere via scattering and absorbing shortwave and longwave radiation (Sokolik et al., 2001). Once deposited in the ocean (Duce et al., 1980), aeolian dust is believed to act as a source of nutrients which cause changes in the primary production of phytoplankton. This process is one of the major factors in the carbon dioxide cycle on a global scale (Duce et al., 1991; Dayan et al., 1991). In addition, phytoplankton on the ocean surface are a biogenic source of sulfate particles in the atmosphere via dimethyl sulfide (DMS) emission. These sulfate particles are activated as cloud condensation nuclei over the ocean and are one of the indirect effects of radiative forcing. However, significant uncertainties remain in understanding the whole dust process, including generation, long-range transport, deposition, and chemical and physical properties, as well as in the model representations of dust distribution and its RF on the global and/or regional scale.

In addition to the climatic issue caused by aeolian dust, dust and sandstorm (DSS) are a serious environmental phenomenon in source regions. In Northeast Asia, more than a hundred million people are affected by DSS. Dust and sandstorms, DSS, are a long-range, transboundary environmental problem in East Asia.

With this background, the Japan–China joint project, Aeolian Dust Experiment on Climate impact (ADEC) was initiated in April 2000 (Mikami et al., 2002). The five-year project consisted of field experiments conducted from March 2001 to March 2005, including three intensive observation periods in 2002, 2003, and 2004. The research sites were located from the source region of the Taklimakan Desert in northeast China to Japan. The research area was widely spread, about 6000 km from west (80°E) to east (140°E), to facilitate monitoring of aeolian dust processes, including emission, long-range transport, and deposition (Fig. 2). The goal of this project is to understand the impact of aeolian dust on the climate system via the direct effect of RF.

This paper intends to provide an overview of ADEC activities and their scientific outcomes. In Section 2, we will describe the outline of ADEC. In Section 3, experimental results regarding wind erosion process, long-range transport process, dust aerosol characterization, and optical properties of dust particles are summarized. Model experiments on dust outbreak mechanisms in East Asia, dust distribution in the global scale, and its radiative forcing effect are also described here. In Section 4, problems related to direct and indirect effects of radiative forcing due to dust are discussed, based on the

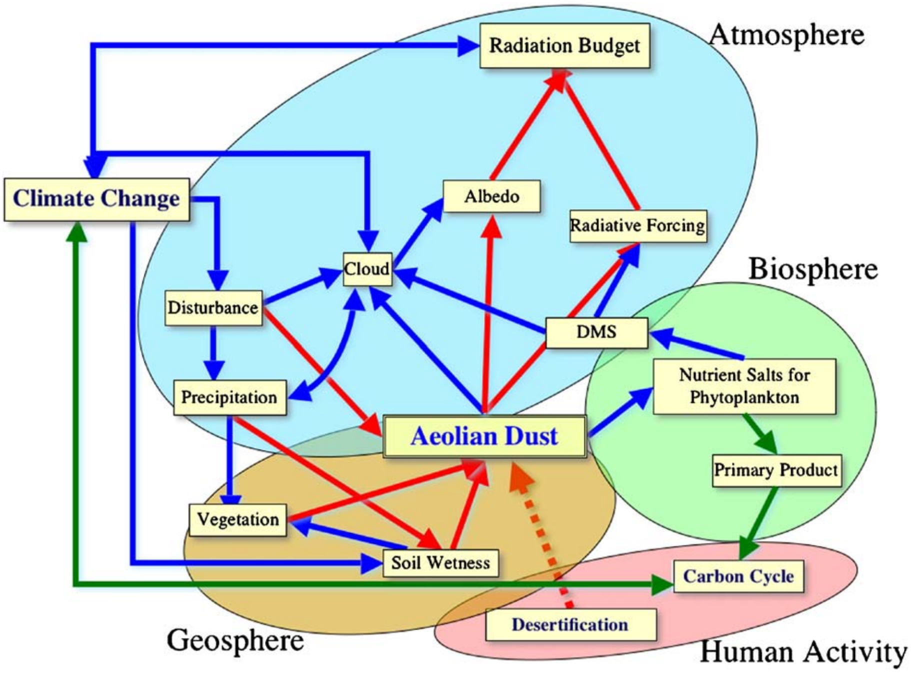

Fig. 1. Schematic diagram of the relation between the earth's climate system and aeolian dust.

experimental findings and model results. Future research issues on dust are also discussed here.

2. Aeolian Dust Experiment on Climate Impact (ADEC)

2.1. Research strategies

For the evaluation of RF due to the direct effect of dust aerosols, large uncertainty still remains (IPCC, 2001). The reasons for the uncertainty derive from the lack of information on the wind erosion processes. Such information will provide data for the validation of wind erosion theory and parameterization for use in a dust model; and also data on the characteristics of dust particles: number, size, physical, chemical, and optical characteristics. In addition, the current dust model can be improved (Uno et al., in press), with the acquisition of better validation data.

For these reasons, we conducted field experiments and numerical simulations to understand the following processes:

(1) wind erosion;
(2) dust concentration, vertical distribution, and deposition;
(3) characterization of aeolian dust: physical, chemical, and optical properties; and
(4) climatic impact of aeolian dust via the direct effect of RF.

To understand the above processes, we developed instruments, tools, and numerical models and implemented a dust monitoring network in East Asia. The following activities were undertaken:

(1) we developed the Sand Particle Counter (SPC) for monitoring moving sand and the Optical Particle Counter (OPC) for monitoring dust particles on the desert surface (Du, 2002; Yamada et al., 2002; Mikami et al., 2005a) to improve the erosion process in the dust model.
(2) we built a lidar monitoring network from the source region in northwestern China to Japan (Fig. 2; Yasui et al., 2002, 2005a; Kai et al., 2005) to monitor the vertical distribution of dust.
(3) we used sky-radiometers for monitoring dust optical properties (Uchiyama et al., 2005a,b). High and low volume aerosol samplers for analyzing the dust particle characteristics (Yabuki et al., 2002, 2005a; Kanai et al., 2005) were placed at the same sites as the lidars and a cascade impactor in an unmanned radio-controlled airplane was used for measuring atmospheric dust particle characteristics at Dunhuang (40° 08′N, 94° 30′E), China, and Mt. Rizan, southwestern Japan (Yamashita et al., 2005).

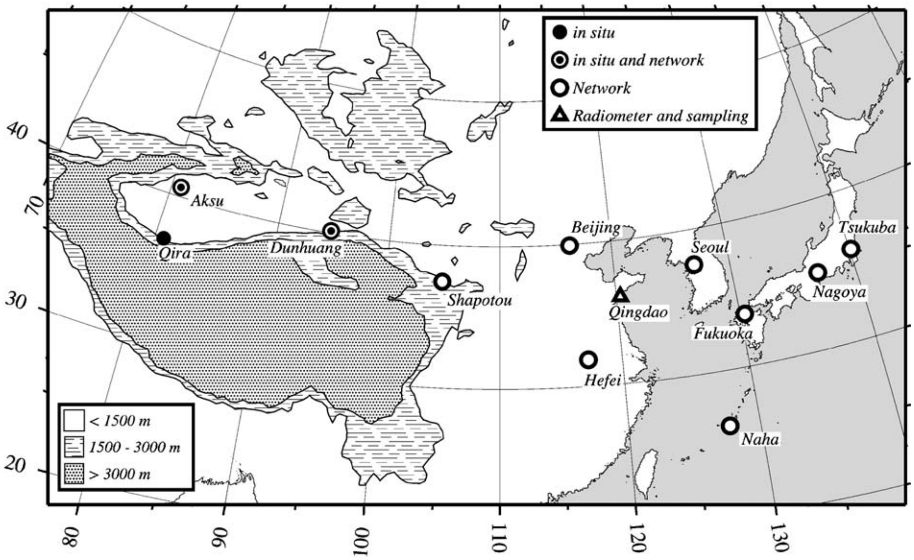

Fig. 2. Map of the ADEC in situ and network observation sites (from Mikami et al., 2005a with permission from American Geophysical Union).

(4) we analyzed the time series of the horizontal distribution of dust aerosol optical thickness derived from the GMS-5 (GMS: Geostationary Meteorological Satellite; Masuda et al., 2005) to monitor the horizontal distribution of dust in East Asia.

(5) we developed two categories of dust model; regional scale models for understanding dust outbreaks and their transport processes and a global scale dust model for the evaluation of the direct effect of RF due to dust. We developed three regional scale models according to their target horizontal scale: a meso-scale model (Takemi, 2005) to investigate dust storm structure and dust uplift mechanism; a local circulation model (Seino et al., 2005) to investigate the mechanism of dust storm events in the Tarim Basin; and a regional-scale dust model (Uno et al., 2005a) to investigate East Asian dust outbreak and its three dimensional distribution within the troposphere. For the evaluation of the direct effect of RF, we developed a global scale dust model (MASINGAR; Tanaka et al., 2005) to investigate global dust distribution and it included a spectrally detailed radiative transfer model (Aoki et al., 2005b).

2.2. Field research plan

The ADEC project established a network of in situ observations, ground-based sampling, sky-radiometer measurements, and lidar observations at 10 sites from the Taklimakan Desert to Japan (Fig. 2). Each site was chosen for monitoring the history of dust aerosols from emission to deposition. Table 1 shows the specifications of the observation at each site.

Three intensive observation periods, April 2002 (IOP1), March 2003 (IOP2), and March to April 2004 (IOP3), were conducted at 6 sites in China (Qira, Aksu, Dunhuang, Shapotou, Beijing, and Qingdao) and 4 sites in Japan (Naha, Fukuoka, Nagoya, and Tsukuba). During these periods, in situ observations for monitoring dust events and erosion processes were conducted at Qira, south of the Taklimakan Desert, and Dunhuang and network observations were conducted to monitor the long-range transport process of dust.

In conjunction with the field experiments, a global dust model, MASINGAR (Tanaka et al., 2003), provided forecast information of dust distribution in northwestern China to support the daily field experiment plan during ADEC IOPs. The daily model forecast information, meteorological satellite image, and surface present weather reports (SYOP; WMO, 1974) in East Asia were provided to field researchers through the ADEC web site to support the fieldwork.

3. Results

The general features of dust storm events in northwestern China during IOP1 (2002) and IOP2 (2003) were considerably different. In the southern Taklimakan Desert, from winter 2001 to spring 2002, two snowfall events were observed; December 4 2001, and January 15 2002. However, the average volumetric soil moisture

Table 1
Observation at each ADEC network site

Site name	Country	Lat.	Long.	In situ observation		Network observation						References
				Wind erosion	Meteorological Elements	Lidar	Radiometer	Hi-volume sampler	Andersen sampler	Dry deposition	OPC	
Qira	China	37° 01′	80° 44′	O	O		O	O	O	O	O	Mikami et al. (2005a,b), Uchiyama et al. (2005b), Yabuki et al. (2005b)
Aksu	China	40° 37′	80° 44′		O	O	O	O	O	O	O	Kai et al. (2005), Uchiyama et al. (2005b), Yabuki et al. (2005b)
Dunhuang	China	40° 08′	94° 41′	O	O	O		O	O	O	O	Du (2002), Iwasaka et al. (2003a), Uchiyama et al. (2005b), Yabuki et al. (2005b)
Shapotou	China	37° 28′	104° 60′		O	O	O	O	O		O	Yasui et al. (2005b), Uchiyama et al. (2005b), Yabuki et al. (2005b)
Beijing	China	39° 56′	116° 21′					O	O			Zhang and Iwasaka (2005), Uchiyama et al. (2005b), Kanai et al. (2005)
Qingdao	China	36° 01′	120° 20′				O	O	O			Zhang and Iwasaka (2005), Uchiyama et al. (2005b), Kanai et al. (2005), Yabuki et al. (2005b)
Hefei	China	31° 54′	117° 10′			O		O	O			Uchiyama et al. (2005b), Kanai et al. (2005)
Naha	Japan	26° 12′	127° 41′			O	O	O	O			Yasui et al. (2005a), Uchiyama et al. (2005b), Kanai et al. (2005)
Fukuoka	Japan	33° 33′	130° 22′			O	O	O	O			Yasui et al. (2005a), Uchiyama et al. (2005b), Kanai et al. (2005)
Nagoya	Japan	35° 09′	136° 58′			O	O	O	O			Yasui et al. (2005a), Uchiyama et al. (2005b), Kanai et al. (2005)
Tsukuba	Japan	36° 04′	140° 08′			O	O	O	O		O	Sakai et al. (2004), Uchiyama et al. (2005b), Kanai et al. (2005)

Modified from Tanaka and Chiba, 2005 with permission from Meteorological Society of Japan.

at the gobi site in the southern Taklimakan Desert was very low during IOP1 (Fig. 3, Ishizuka et al., 2005). From winter 2002 to early spring 2003, four snowfall events occurred in this region and the soil moisture at the site was considerably higher than in 2002. This resulted in a large difference in the atmospheric loading of dust in IOP1 and IOP2 at source regions in China (Mikami et al., 2005b) and downwind regions in Japan. The 2004 spring season during IOP3 was comparatively normal in northwestern China. During IOP3, however, a widespread dust storm occurred in the northern Taklimakan Desert from 10 to 12 March. This dense dust storm originated in the north of the basin and then moved southwestward. A high number concentration of super-micron particles remained for a long period of time (12 to 28 March) in the south of the basin (Mikami et al., 2005b).

3.1. Wind erosion process

Wind erosion is an essential process of dust emission to the atmosphere; therefore, understanding the process and its parameterization for the dust model is one of the main objectives of this project. To address this issue, basic information on aeolian dust under various meteorological conditions is required (Shao, 2000; Mikami et al., 2002). For this, field experiments were conducted at a sand dune and a gobi (surface with sand and pebble)

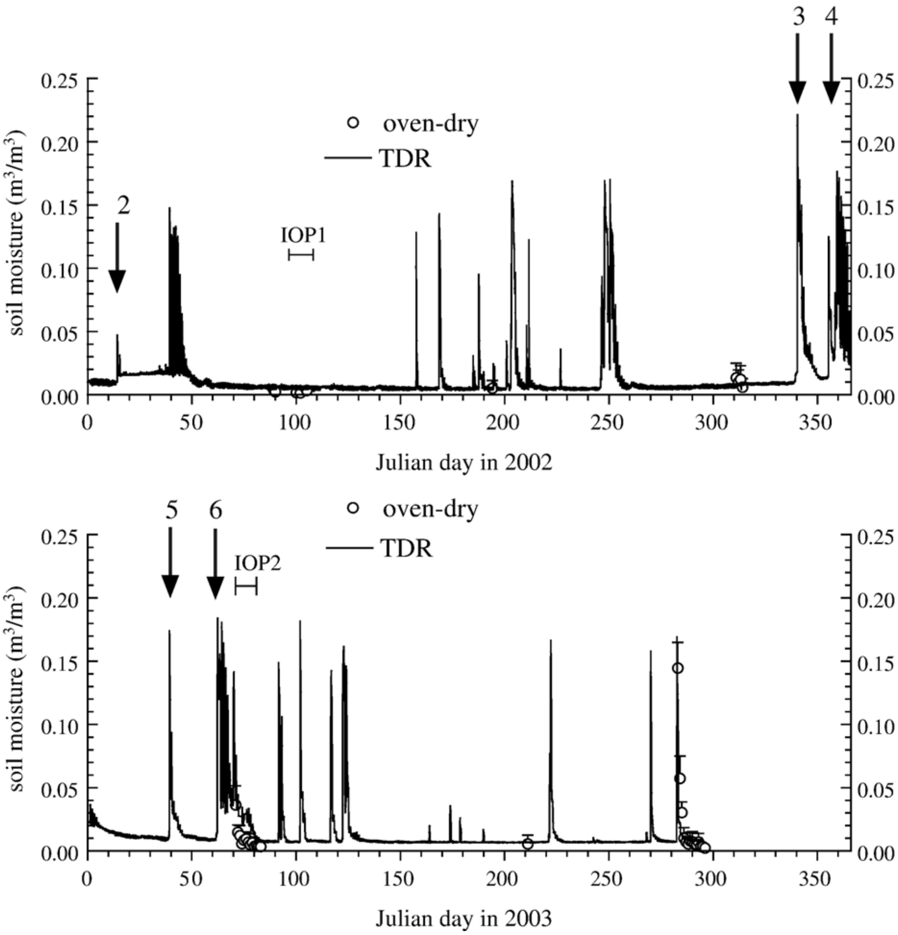

Fig. 3. Long-term soil moisture variation at a depth of 0.01 m in the center of the sampling area at the gobi site near Qira in the Taklimakan Desert. Solid line shows TDR-measured soil moisture (m^3 m^{-3}). Direct sampling data are also plotted (modified from Ishizuka et al., 2005 with permission from American Geophysical Union).

desert in the southern Taklimakan Desert (Mikami et al., 2005a, Ishizuka et al., 2005) and at a gobi desert and a fallow cotton field in Dunhuang, China (Du, 2002). We developed a new sand particle counter (SPC) to monitor heterogeneous saltation (Shao and Mikami, 2005) in the field. The SPC was designed to sequentially measure the saltating sand particle size from 40 to 600 μm at a high time resolution (one second) (Fig. 4; Yamada et al., 2002; Mikami et al., 2005a).

Fig. 5 illustrates the time variations of the saltation particle numbers at 30 cm height in 1 s intervals (thin line) and 21 s moving averages (thick line) on the gobi site in the southern Taklimakan Desert using the SPC (Mikami et al., 2005a). This indicates that the SPC sufficiently represents the detailed saltation process with high time and size resolutions. The threshold wind velocity in the gobi site was 7.5 m s^{-1}, and the total saltation fluxes for the gobi and for the dune during 5 April 2002 (1223 to 1430 UT) were 37.93 and 2.61 kg m^{-2} at 30 cm height, respectively. Thus the saltation flux at the dune site was only 7% of that at the gobi site, although the distance between the sites is only 4 km. The difference is attributed to the parent soil size distributions. It was also found that the particle size distributions at the gobi sites varied with height; that is, the number size distribution of the coarse particles (117 to 554 μm) at 20 cm height was greater than that at 30 cm height (Fig. 6). This is reasonable from a physical viewpoint, because the greater the height, the fewer the number of coarse saltation particles owing to the gravitational effect. However, the present saltation theory cannot thoroughly explain this particle size dependency with height.

Ishizuka et al. (2005) analyzed streamwise saltation flux of multi-sized soils, $q(z;\ d)$, for particle size d from 38 to 667 μm with 32 bins for different soil

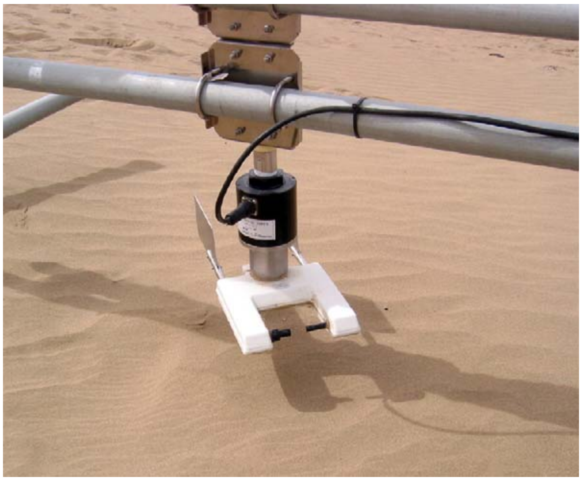

Fig. 4. Sand particle counter (SPC) installed on the dune site in the southern Taklimakan Desert, China.

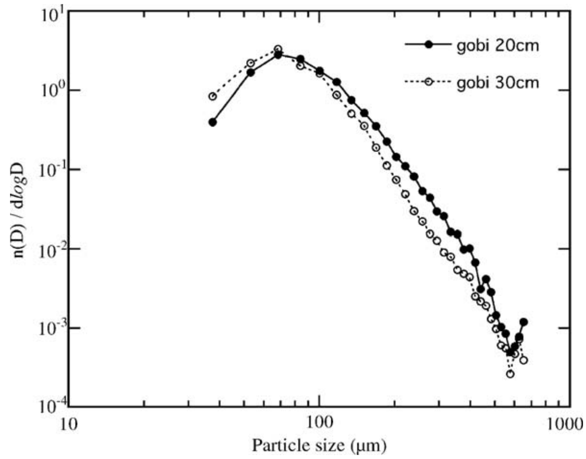

Fig. 6. Particle size distribution of the saltation particles. Relationship between the gobi sites for 20 and 30 cm height (from Mikami et al., 2005a with permission from American Geophysical Union).

moisture conditions on the gobi site. The threshold wind speed $u_t(\theta)$ for wet conditions ($\theta = 0.009$ m^3 m^{-3}) was estimated to be 9.5 m s^{-1} at 3.8 m height and was 1.27 times greater than that for dry conditions ($\theta = 0.002$ m^3 m^{-3}), which corresponds to the theoretical consideration of Fe´can et al. (1999). The soil moisture had marked effects on the threshold wind speed u_t and q. It was also demonstrated that (1) the saltation flux, $\hat{q}(d)$, for different particle size d for coarse sand particles of 69 to 203 μm in diameter in wet condition were smaller than those in dry condition; whereas, the $\hat{q}(d)$ for fine sand particles of 39 to 54 μm did not change and (2) the saltation particle size spectra changed from dry to wet conditions. These results suggest that the q depends on particle size and soil moisture.

3.2. Dust storm outbreak and aeolian dust transport process in East Asia

3.2.1. SYNOP analysis

Annual and long-term trend of dust outbreak in East Asia and/or China have been discussed widely to date (Yoshino, 2002; Kurosaki and Mikami, 2003; Zhao et al., 2004; Ding et al., 2005). Despite this, we do not have a clear understanding of the statistical evidence of the recent dust outbreaks. Quantitative assessment is difficult because the present weather and visibility reports were made by visual observations. In order to clarify the recent dust events in East Asia, Kurosaki and Mikami (2003) analyzed the relationship between dust outbreaks and strong winds using present weather reports and the surface wind velocity obtained from a SYNOP report for

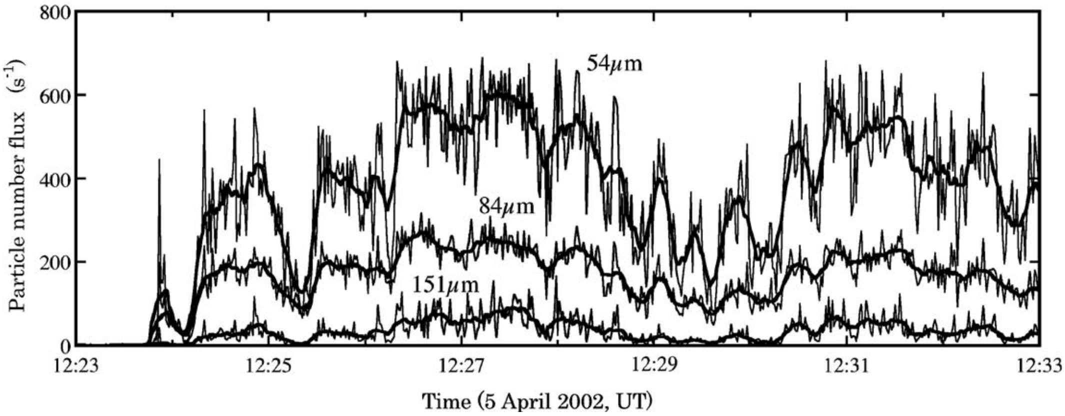

Fig. 5. Time variations of the saltation particle numbers in 1-s intervals (thin lines) and 21-s moving averages (thick lines) at 30 cm height for the gobi site from 1223 to 1233 UT, 5 April 2002 (modified from Mikami et al., 2005a with permission from American Geophysical Union).

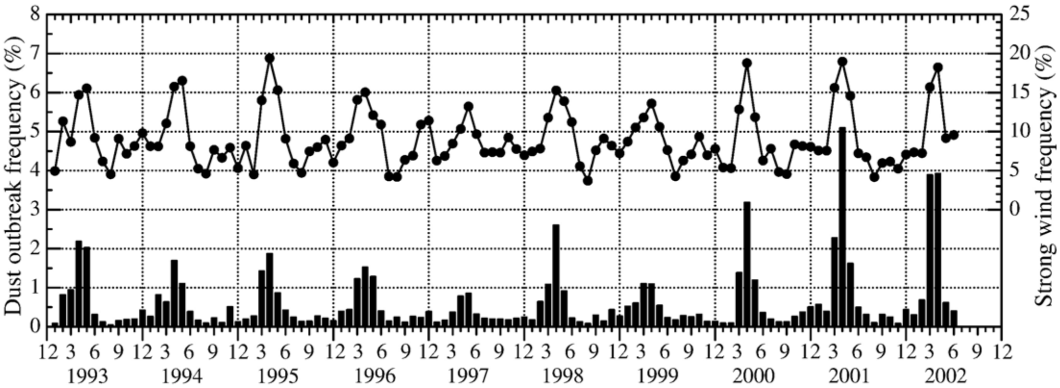

Fig. 7. Monthly dust outbreak frequency and strong wind frequency from Jan. 1993 to Jun. 2002. The black bar chart and line graph with black dots indicate dust outbreak frequency and strong wind frequency (modified from Kurosaki and Mikami, 2003 with permission from American Geophysical Union).

the period 1993 to 2002. They showed that the dust outbreak frequency in East Asia has large annual variability and that there was a notable increase in dust outbreaks in the eastern part of the Asian continent for the three years from 2000 to 2002 (Fig. 7). They also found a good relationship between the surface wind (strong wind frequency) and dust outbreaks (frequency of dust outbreak) in year-to-year variations and in spatial

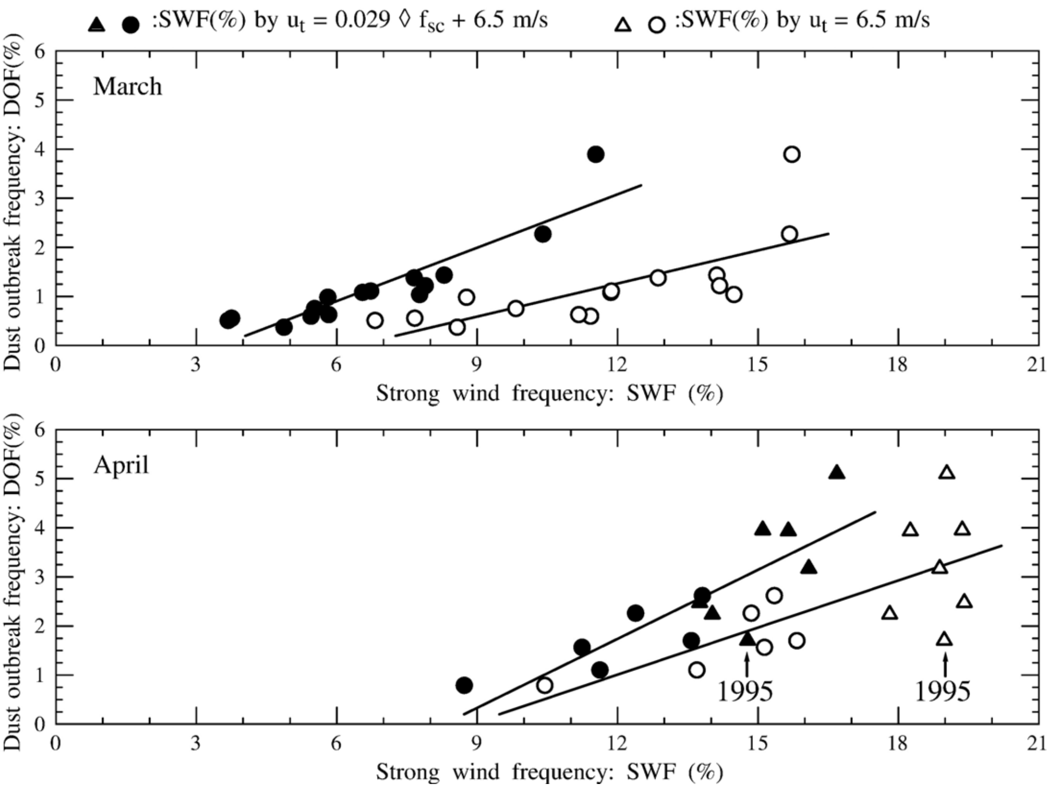

Fig. 8. Relationship between the SWF and the DOF in March (upper panel) and in April (lower panel) for each year from 1988 to 2003. Two types of SWFs are shown. For the SWFcnst (white circles and triangles), a strong wind is defined by a constant value, 6.5 m/s. For the SWFvar (black circles and triangles), a strong wind is defined by Eq. (1). Neither white nor black symbols are shown for March 1991 and April of 1991, 1993, and 1996 because there is no snow cover data for these periods (modified from Kurosaki and Mikami, 2004 with permission from American Geophysical Union).

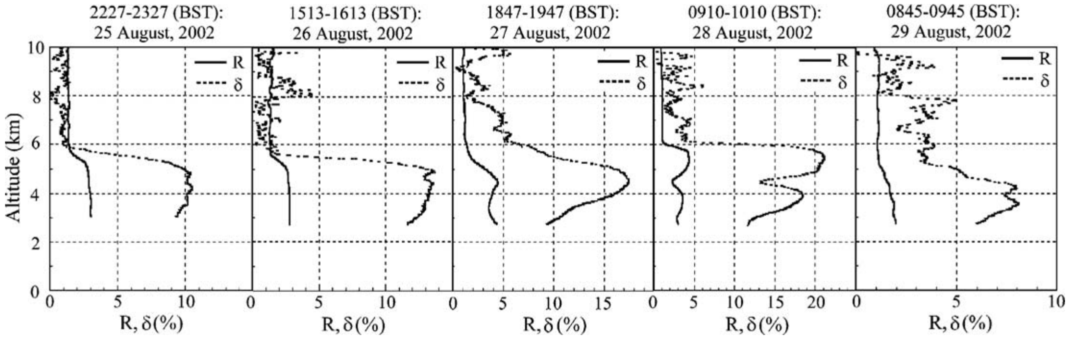

Fig. 9. Vertical profiles of backscattering ratio (R) and depolarization ratio (d%) measured at Dunhuang, China (from Iwasaka et al., 2003a with permission from American Geophysical Union).

distributions. This indicates that frequent strong winds are the primary cause of the recurrent dust outbreaks in the last three years.

Kurosaki and Mikami (2003) also demonstrated the degree to which snow cover affects dust outbreaks. They evaluated the correlation coefficients between frequency of strong winds and dust outbreaks and found that this correlation improves when the effect of snow cover is considered (Fig. 8). They proposed an equation representing the degree to which snow cover affects dust outbreaks. When a threshold wind velocity under no snow cover condition is set as u_{t0}, a threshold wind velocity under snow cover condition (u_t) can be expressed as,

$$u_t = r \times f_{sc} + u_{t0} \tag{1}$$

where r is the increase rate (0.027 to 0.030), and f_{sc} is a snow cover fraction. This snow cover effect was apparent in East Asia during early spring from March to April for the past 10 years, 1993 to 2002.

3.2.2. Lidar observation

Lidar is a useful method for remote aerosol measurements. It measures the vertical distributions of the aerosol backscatter/extinction coefficients and the backscattering depolarization ratio. The depolarization ratio can be used to distinguish the dust from the other aerosol species and clouds because it is a measure of the particles' nonsphericity. During ADEC IOPs, eight lidar sites, from the Aksu, an outbreak area located in the northern Taklimakan Desert, to Japan, were installed to monitor aeolian dust outbreak and its long-range transportation (Table 1; Mikami et al., 2002; Yasui et al., 2005a).

Lidar measurements made at Dunhuang revealed that non-spherically shaped dust particles floated from near the surface to about 6 km (Fig. 9; Iwasaka et al., 2003a). This was supported by the aerosol vertical profile measured with a balloon borne optical particle counter, as well as by the analysis of the particles collected in the free troposphere with a balloon borne particle impactor (Fig. 10). The electron microscopy on the collected individual particles directly demonstrated that the mineral dust particles were the major constituents of the coarse mode particles in the free troposphere over the Taklimakan Desert (Iwasaka et al., 2003b). Yasui et al. (2005b) also observed a thick and dense dust layer at heights between 1.5 and 5 km above MSL at Fukuoka, in the southern part of Japan, during ADEC IOP1. Raman lidar measurements during the dust event on 23 to 24 April 2001 over Tsukuba, in the middle part of Japan,

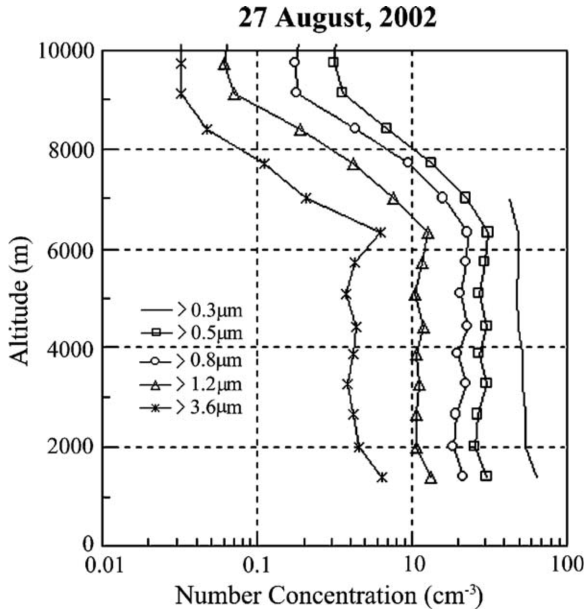

Fig. 10. Particle number concentration measured with an optical particle counter on 27 August 2002 at Dunhuang, China (from Iwasaka et al., 2003a with permission from American Geophysical Union).

revealed the presence of dust layer at an altitude range of 6–9 km (Sakai et al., 2004). These observations show that dust layers can be found in the middle to upper free troposphere from the dust source to downwind regions in East Asia.

Using the lidar information as a tracer of the atmosphere, Yasui et al. (2005b) investigated the structure and the diurnal change of a dry convective boundary layer developed over the arid region in Shapotou, Ninxia Province in China. They found that the deepest mixed layer of 6 km above the ground surface formed under weak wind shear and dry atmospheric conditions.

3.2.3. Modeling of dust emission and transport processes over East Asia

The Taklimakan Desert is undoubtedly one of the strongest dust source regions in East Asia. Recently, Bory et al. (2003) showed that dust from the Taklimakan Desert was deposited in Greenland. This implies that the horizontal and vertical dust emission and distribution of Asian dust are a matter of concern not only for understanding the atmospheric environment in East Asia but also for understanding dust impact on the climate on a global scale. However, when ADEC was initiated, only a few modeling studies had been undertaken for East Asia, especially from the Tarim Basin (e.g. Wang et al., 2000; Uno et al., 2001). In the ADEC program, as is described in Section 2.1, three models were used for understanding dust outbreaks and their transport from East Asia: (1) a cloud resolving meso-scale dust model (Takemi, 2005; Takemi et al., 2005), (2) a local circulation model (Seino et al., 2005), and (3) an East Asia regional scale dust model (Uno et al., 2005a).

Takemi (2005) explicitly simulated the convective-scale transport of mineral dust in a severe weather setting with the approach of three-dimensional cloud-resolving simulations coupled with a dust emission-transport model. He simulated the dust emission process followed with a squall-line-type convective system as follows. (1) Dust is emitted by strong surface winds associated with a well-developed surface cold pool, and is contained and mixed within the cold pool, inducing a high dust concentration exceeding 10 mg m^{-3}. (2) Due to high subgrid-turbulence mixing at the leading edge of the cold pool, the contained dust is transferred out of the cold pool and is entrained into the updraft region at the cold pool edge. (3) Dust is then transported upward by the convective updraft that is continuously regenerated at the cold-pool leading edge, and spreads laterally in the cross-line directions at upper levels by system-scale circulation. (4) Rearward dust transport relative to the leading edge of the system is pronounced at upper levels, according to the prevalent front-to-rear flow typically found in the squall-line systems.

Based on the regional climate model with a grid size of 20 km developed by MRI/JMA, Seino et al. (2005) conducted numerical simulations of meso-scale circulation in the Tarim Basin for a dust event on 12 to 15 April 2002. They validated the model results with observed surface wind and significant weather around the region and the model reasonably simulated the time variations and spatial distributions of the surface wind field during this event (Fig. 11). The simulation revealed three types of meso-scale flow within the basin. Sequential formation and/or coexistence of these flows can cause wind intensification and active dust emission from various areas across the basin. They demonstrated a close relationship between development of these meso-scale circulations and the large-scale flow field behind the low-pressure system.

Uno et al. (2005a) developed a nested regional meteorology/dust-transport model to examine the typical springtime meteorology and dust outbreak over the Taklimakan Desert region. The model results reproduced complicated airflows within the Tarim Basin, strong down slope winds from the Tianshan Mountains when meteorological disturbances cross over the Taklimakan region, and a strong easterly flow from the Hexi Corridor side. The scale of this strong easterly wind zone is 400 km from north to south, 1000 km from east to west and 2 to 3 km vertically. The simulated high dust concentration correlated well with this easterly wind zone.

CFORS was also used for the long-term simulation of Asian dust aerosol to reveal major inter-annual variation of dust event activity (Hara et al., 2004). Although the ground surface conditions of the model domain were fixed during its long-term simulation, the results adequately reproduced major inter-annual variation of observed dust (Fig. 12). This implies that meteorological condition is a stronger driver of dust event than land surface condition.

3.3. Dust aerosol characterization

There are several different methods and instruments for characterizing dust aerosol. In the ADEC project, we adopted Andersen low-volume air samplers with eight-stage impactor plates and high-volume air samplers for ground level observation of aerosols from the source region, the Taklimakan Desert, to the downwind area, eastern China and Japan. Dry depositions were also collected using dry deposition samplers (Sibata Scientific Technology Ltd., Dry Deposition Sampler). Those

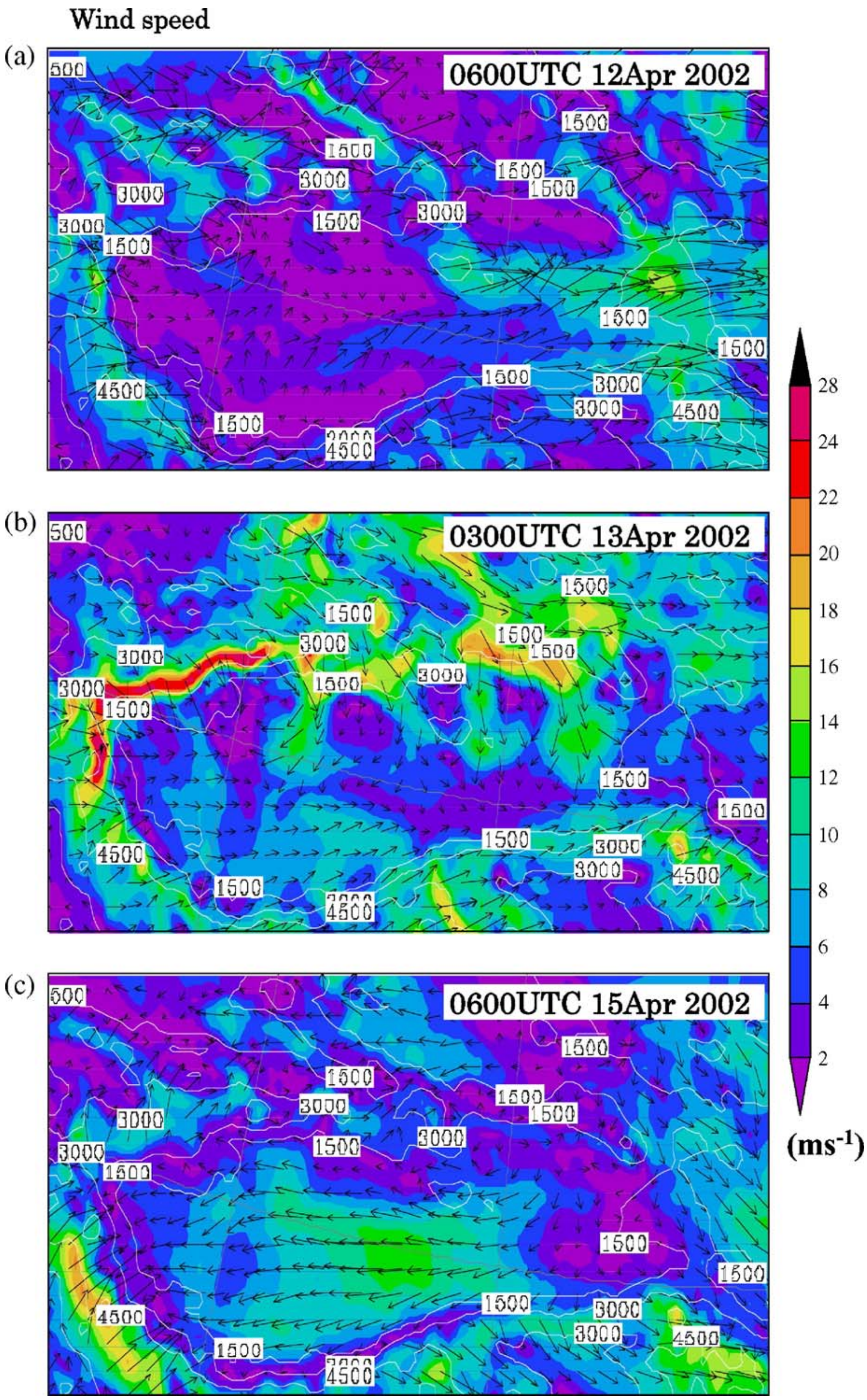

Fig. 11. Simulated surface wind in the Tarim Basin at (a) 0600 UTC 12, (b) 0300 UTC 13 and (c) 0600 UTC 15 April 2002. Topographic contours are drawn at 1500 m intervals. Longitude/latitude lines are also shown every 10° (modified from Seino et al., 2005 with permission from Meteorological Society of Japan).

samplers were operated over a long period from March 2001 to April 2004 for monitoring seasonal and annual variation of dust concentration, TSP (total suspended particles) and PM_{11} (particles < 11 μm), and size information at each network site (Fig. 2). The TSP and PM_{11} concentrations show the average concentration

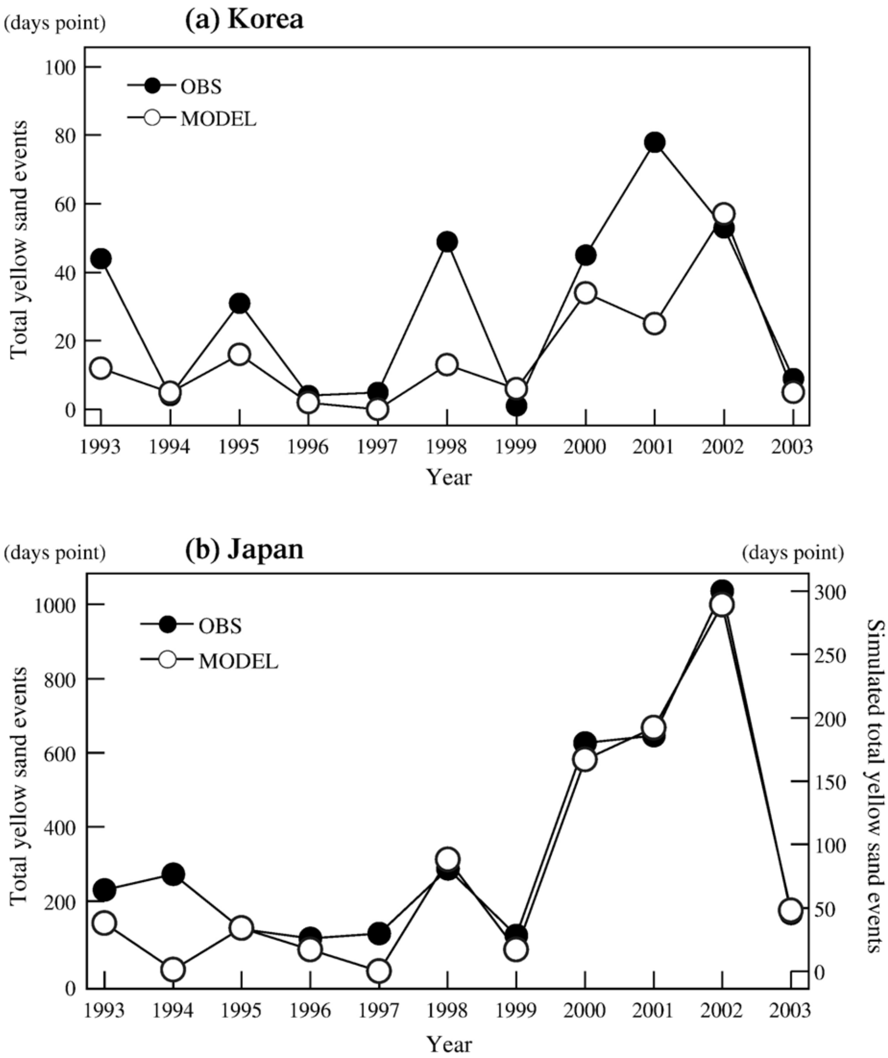

Fig. 12. Annual variation of yellow sand (Kosa) count in Korea and Japan. Solid circles indicate an observation. Open circles are simulated Kosa counts based on the dust transport model simulation.

during the sampling period, and the sampling frequency is once or twice a month with a sampling duration of a few days to one week, so sampling period does not necessarily overlap dust events. As dust events are most frequent during spring, we conducted three intensive observation periods, from 11 to 24 April in 2002, from 16 to 26 March in 2003 and from 10 to 17 March in 2004, during which sampling is only interrupted for filter changes. Collected samples were also used for mineralogical, chemical and isotopical analysis.

Particles of up to 8600 m of free troposphere were also collected with an aircraft-borne or balloon-borne particle impactor over the desert areas in China and over Japan (Iwasaka et al., 2003b). In situ observations and sampling of aerosol particles in the upper mixed layer and lowermost free troposphere were carried out using a multi angle optical particle counter (MAC, Hayashi et al., 2005) and a cascade impactor mounted on an unmanned airplane over Dunhuang, China and Mt. Raizan, southwestern Japan (Yamashita et al., 2005).

3.3.1. Concentration and physical/chemical characteristics of dust over source region

Yabuki et al. (2005a,b) summarized aerosol characteristic from ground based observations at four observation sites, Qira (37° 01′ N, 80° 44′E), Aksu (40° 37′ N, 80° 44′E), Dunhuang (40° 08′N, 94° 41′E), and Shapotou (37° 28′N, 104° 60′E), over Asian dust source areas.

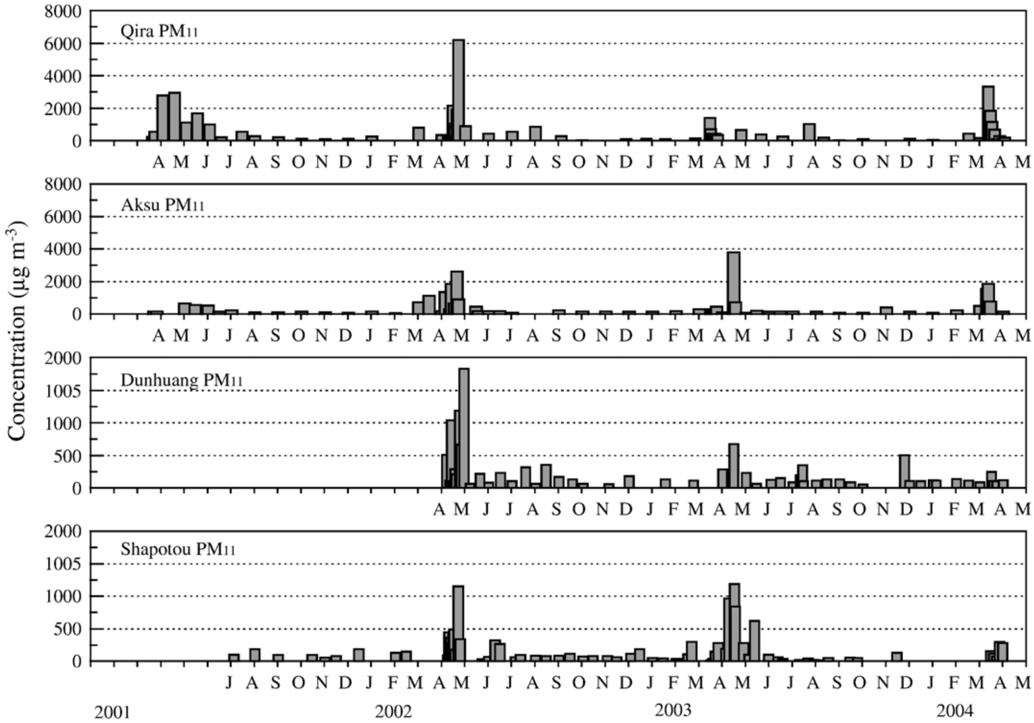

Fig. 13. Variation of PM_{11} concentration at each observation site: from April 2001 to March 2004 for Qira and Aksu, April 2002 for Dunhuang, and July 2001 for Shapotou (from Yabuki et al., 2005a).

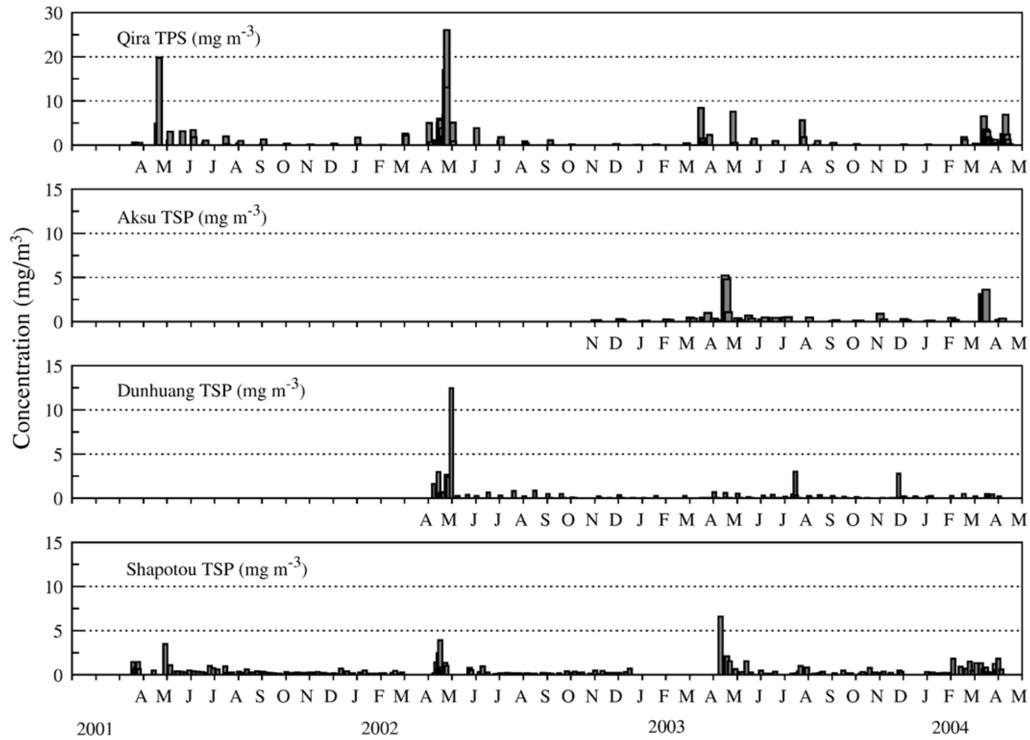

Fig. 14. TSP concentration at four observation sites from April 2001 for Qira and Shapotou, from November 2002 for Aksu and from September 2001 for Dunhuang to March 2004 (from Yabuki et al., 2005a).

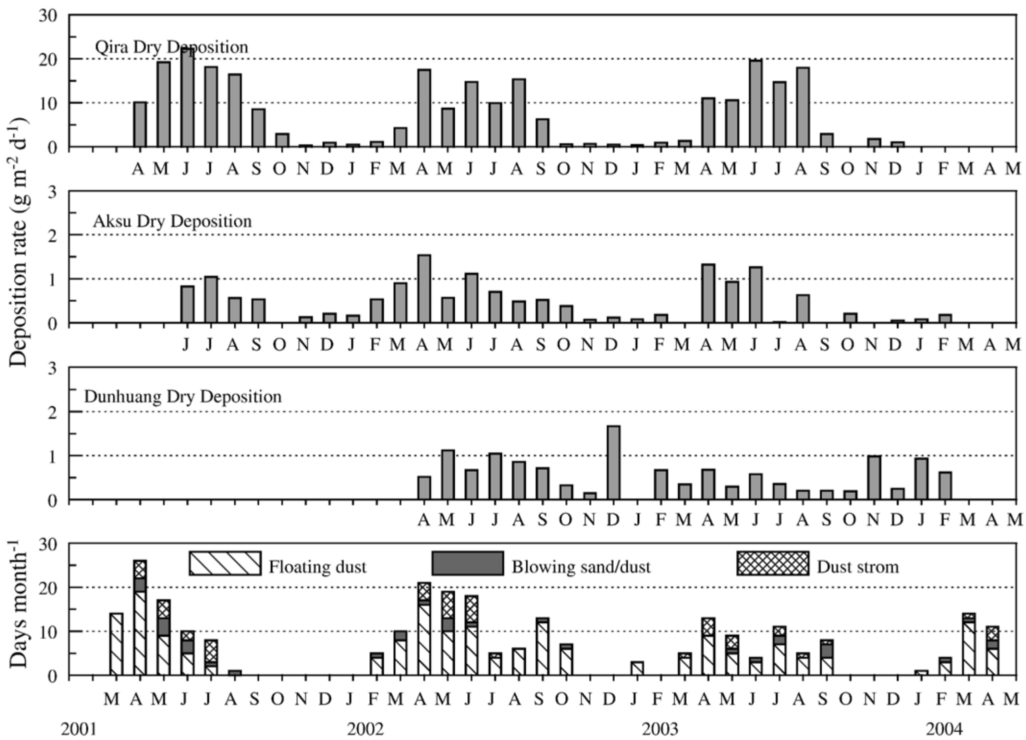

Fig. 15. Dry deposition rate from April 2001 at Qira, from May 2001 at Aksu, and from April 2002 at Dunhuang together with dust event frequency at Aksu (from Yabuki et al., 2005a).

Fig. 13 shows the variation of PM_{11} concentration (sum of particles less than 11 μm stages of Andersen samplers) for four observation sites. In Fig. 14, total suspended particle (TSP) concentration at four observation sites from April 2001 for Qira and Shapotou, from November 2002 for Aksu and from September for Dunhuang to March 2004 are shown. Dry deposition rate from April 2001 at Qira, from May at Aksu, and from April 2002 at Dunhuang together with dust event frequency at Aksu are shown in Fig. 15. Sampler breakdown caused loss of some data. It is obvious that high PM_{11} and TSP concentrations are observed during spring; however, dry deposition was observed not only in spring but also during summer or fall. In Fig. 15, dry deposition rates at Qira are more than 10 times higher than Aksu and Dunhuang, while TSP and PM_{11} concentration is only a few times higher than at other observation sites. These extraordinarily high dry deposition rates at Qira probably result from the desert environment around the observation site. As mentioned above, Qira is situated at the border of Taklimakan Desert, while Aksu and Dunhuang are situated almost inside oases. Although Shapotou is also at the border of Tengger Desert, the TSP concentration or dry deposition rate were the lowest of the four observation sites.

In China, dust events are classified into three categories, dust storm (wind speed > 10 m/s, visibility < 1 km), blowing dust/sand (wind speed > 5 m/s, visibility: 1–10 km) and floating dust (wind speed > 5 m/s, visibility: < 10 km). Fig. 16 shows the typical size distribution pattern for three categories in Qira. Coarser particle (> 11 μm) concentration is highest in dust storm and blowing dust/sand samples in Qira. Size distributions of the TSP samples collected during dust storm and floating dust at Qira are shown in Fig. 17. Cumulative percentage of particles smaller than 10 μm diameter is 53.5% for floating dust sample, while it is only 2.4% for dust storm sample. The traveling distance and lifetime of dust particles in the atmosphere depend on the particle size (Tsor and Pye, 1987; Tanaka and Chiba, 2005). Accordingly, it is suggested that the coarse particles of TSP or dry deposition are mostly of local origin.

With regard to major element composition, aeolian dusts are low in SiO_2 and high in Fe_2O_3, K_2O, and MgO when compared with reference surface soils, such as saline soils around the observation site, the Loess

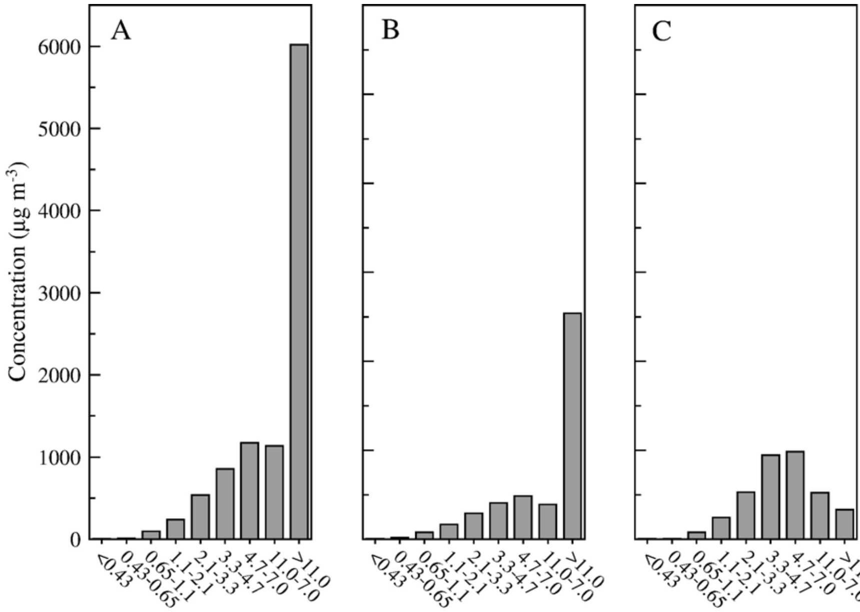

Fig. 16. Size distribution of aerosol particles during different dust events at Qira. A: Dust storm. B: Blowing dust/sand. C: Floating dust (from Yabuki et al., 2005a).

deposits and the desert sands. This suggests that minerals rich in K, Fe, and Mg, such as mica or clay, are selectively transported from the soil surface into the atmosphere. Major soluble ions of aerosols are Na^+, Ma^{2+}, Ca^{2+}, NH_4^+, Cl^-, NO_3^-, and SO_4^{2-} ions. Ca^{2+}, Na^+, and Cl^- have unimodal distributions with a peak in the 3.3 to 7.0 μm range; NH_4^+ also has a unimodal distribution with a peak in the submicron range. NO_3^- and SO_4^{2-} have bimodal distributions with peaks in the micron and submicron ranges, especially during winter. Soluble Na^+ and Cl^- are produced from sodium chloride (halite), Ca^{2+} is produced from calcium carbonate (calcite) and calcium sulfate (gypsum and anhydrite). Anthropogenic ammonium sulfate and ammonium nitrate were observed in the 0.65 to 1.1 μm region, especially during winter. It is suggested that

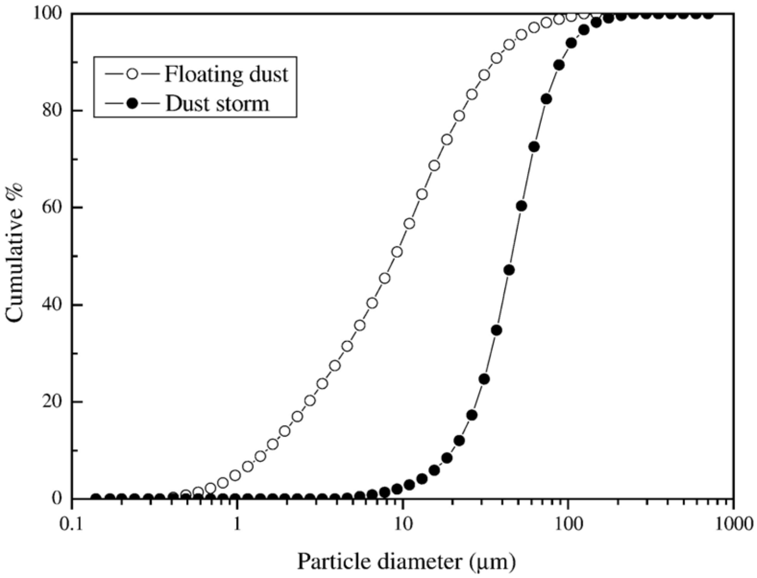

Fig. 17. Size distribution of TSP during floating dust and dust storm at Qira (from Yabuki et al., 2005a).

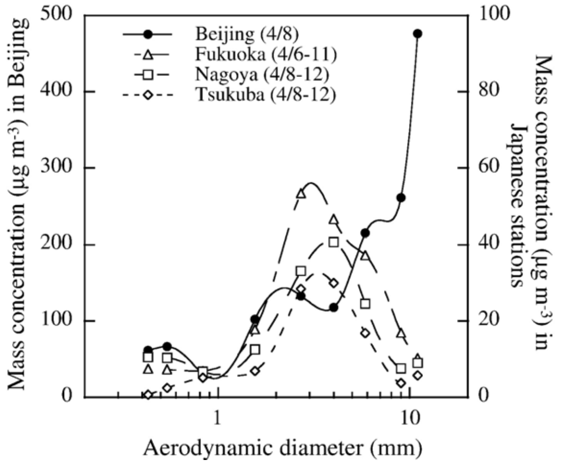

Fig. 18. Distribution of mass concentrations of aerosol collected at Beijing, Fukuoka, Nagoya and Tsukuba when a large-scale dust event was observed (6–12 April 2002) (from Ohta et al., 2005).

these anthropogenic pollutants result mainly from local coal combustion.

3.3.2. Concentration and physical/chemical characteristics of dust at downwind area from source

Total suspended particle (TSP) and size-segregated dust concentrations were monitored in Beijing, Qingdao and Hefei in China, and in Fukuoka, Nagoya, Tsukuba, and Naha in Japan (Kanai et al., 2005). The aerosol concentrations were high in spring and low in summer at every site, though it sometimes became high in the winter in Qingdao, which might be due to the increase of coal combustion during winter season. The aerosol size distributions were bimodal at every site. One peak at around 0.5 μm diameter corresponded to particles of anthropogenic origin, in which the main components were black carbon, NH_4^+ and SO_4^{2-}, and some elements such as Pb, Cd, Sn, Sb, and Bi were abundant. The other peak at 4 to 5 μm diameter corresponded to mineral dust of soil origin, in which the main soluble components were Na^+, Ca^{2+}, NO_3^-, and Cl^-.

Chemical characteristics of dust were analyzed during a large-scale dust event from 6 to 12 April 2002 using samples collected in Beijing, Fukuoka, Nagoya, and Tsukuba (Ohta et al., 2005). Fig. 18 shows aerosol concentrations in Beijing, Fukuoka, Nagoya, and Tsukuba. Total dust concentrations decrease in the order of Beijing, Fukuoka, Nagoya, and Tsukuba. Beijing is characterized as having the highest dust concentration for coarse grains (over 7 μm), which is similar to those of dust samples collected at source region, Qira and Shapoutou (Yabuki et al., 2002). Three Japanese stations show that the distribution has bimodal peaks at 2.1–7.0 μm and 0.43–0.65 μm. The fine grain consists mainly of carbon aerosol and shows a strong local aerosol contribution. The metal/Al concentration ratios indicate no change in chemical compositions in aerosol between Beijing and Japanese stations. X-ray absorption near-edge structure (XANES) spectroscopic study reveals that the oxidation–reduction reaction of Fe and Mn in aeolian dust during its transportation from China to Japan is negligible. Some aeolian dust elements, such as Zn and Pb, were enriched in fine ($d<2.1$ μm) grains, which consist of mainly carbon aerosol and are considered to originate from anthropogenic materials (Fig. 19). However, the Zn XANES spectra for Beijing indicate that Zn in aeolian dust that was collected from this large-scale dust event is present as mineral aerosols and has only a slight contribution from anthropogenic materials.

Lee et al. (2005) attempted to estimate dry deposition during the dust events in spring 2002 (Period I: 15 to 24 March, Period II: 4 to 13 April) using the Asian Dust Aerosol Model (ADAM). The ADAM results and OPC measurements in Anmyendo in Korea correlated well, that is the correlation coefficients between ADAM and OPC were 0.88 (Period I) and 0.64 (Period II) for 1.35–2.23 diameter range and 0.78 (Period I) and 0.54 (Period II) for total deposition. The dry deposition was estimated to be 4.40 ton km^{-2} during Period I and 1.89 ton km^{-2} during Period II over South Korea; 6.59 ton km^{-2} during Period I and 2.51 ton km^{-2} during Period II over North Korea; and 1.52 ton km^{-2} during Period I and 0.41 ton km^{-2} during Period II over Japan.

3.3.3. Isotopic compositions of dust as tracers for source identification

Kanayama et al. (2005) suggested that Sr and Nd isotopic trends are useful for tracing transportation of dust aerosols, because there is obvious isotopic variability among surface soils of possible source areas in Asian dust source regions. Based on the analysis of the chemical and isotopic composition of Sr and Nd in TSP and its finer fraction ($\varphi<5$ μm), and of surface soils of possible source areas, it was suggested that the broad area, from the Taklimakan Desert to the Central Loess Plateau, is characterized as a single possible source component of Asian dust. By comparing isotopic results with the meteorological evaluations for potential sources of dust events, it was noted that the possible sources identified by Sr and Nd isotopic compositions do not correspond to the potential sources identified by the meteorological data, especially in the Beijing case and other areas with abundant dust source materials. To increase the applicability of Sr and Nd isotopes as geochemical

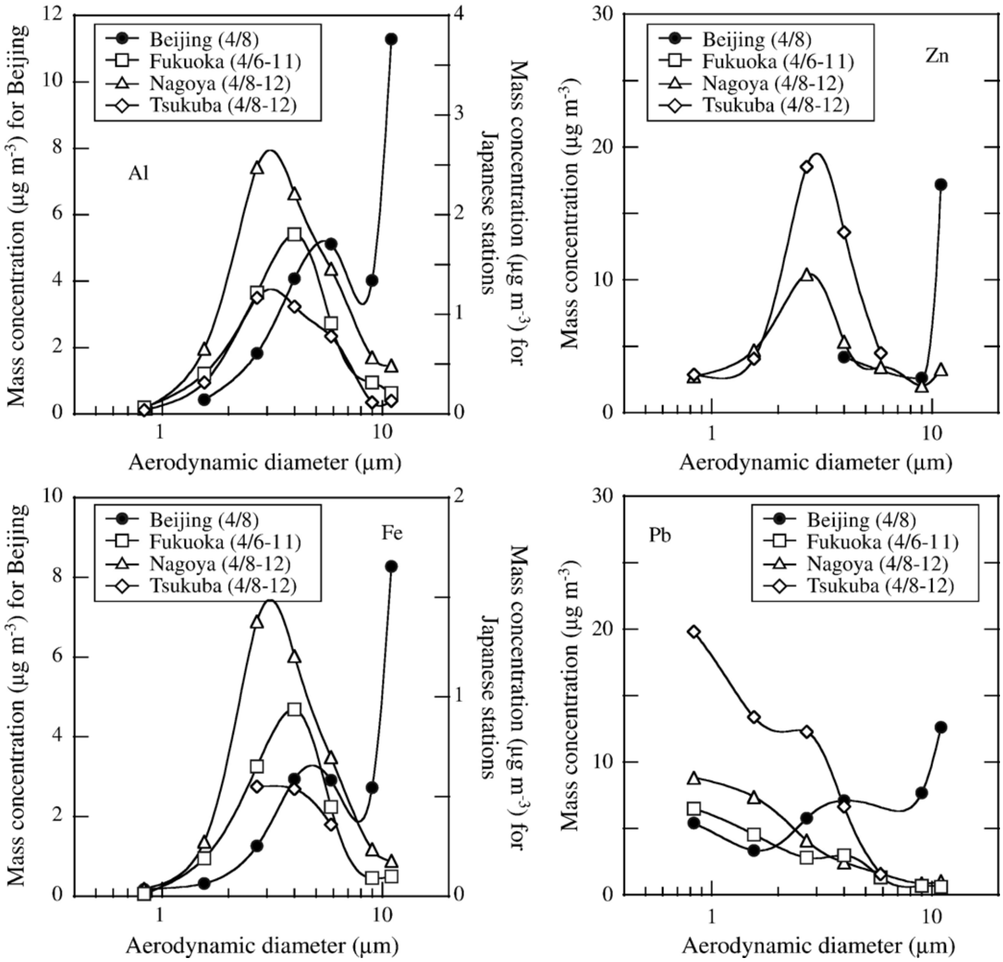

Fig. 19. Distribution of Al, Fe, Zn, and Pb concentrations in dust samples collected at Beijing, Fukuoka, Nagoya, and Tsukuba when a large-scale dust event was observed (6–12 April 2002) (from Ohta et al., 2005).

tracers for Asian dust, further data on the fine fraction of surface soils and dust aerosols must be accumulated.

3.3.4. Mixing of dust aerosol during long-range transportation

The mixture of dust aerosols with anthropogenic particles such as sulfate, nitrates, black carbon, and organic carbon changes the optical and physical properties of dust and affects the climatic impact via direct and indirect effects by dust aerosols. During the ADEC IOPs, analyses were made using a Scanning Electron Microscope with an Energy-Dispersive X-ray analyzer (SEM-EDX) for samples collected at Dunhuang (a dust source region), Beijing and Nagoya (central Japan; Iwasaka et al., 2003b; Matsuki et al., 2005), and at Mt. Raizan (southwestern Japan; Yamashita et al., 2005).

Even though the series of measurements were conducted on days unaffected by severe storms, 95% of coarse particles in the free troposphere (3 to 9 km) over Dunhuang were found to be dust, 35% to 68% in Beijing near the ground (0 to 1 km), and 69% to 90% for the free troposphere (0.5 to 5 km) over Japan (Matsuki et al., 2005). A high level of sulfate was detected in the dust collected in Beijing, downwind from the source, and the heterogeneous uptake of gaseous SO_2, and the subsequent oxidation on dust was suggested to occur in the ambient environment. A positive correlation was also found with the number of sulfate containing particles and the relative humidity.

Yamashita et al. (2005) carried out an in situ sampling of aerosol particles from 800 to 2000 m altitude over Mt. Raizan (33.5 °N, 130.2°E) from March to April 2003 using an unmanned radio-controlled airplane. In the mixed layer, mineral particles, sea salt particles, and their mixture were dominant among the coarse particles, whereas sulfate particles dominated the fine particles. In the free troposphere, mineral particles dominated both the coarse and fine particles. Of all the particles in the mixed layer, the number fractions of mineral particles mixed with sea salt were much higher than those in the free troposphere. This suggests that mineral particles were mixed with sea salt in the marine boundary layer. The weather analysis suggested that the formation process through the clouds, which had previously been considered an efficient formation process for mixed particles, could not sufficiently explain the observed abundance of mineral particles internally mixed with sea salt.

During three dust storm events (April 8, 12, and 27, 2000), Zhang and Iwasaka (2004 and 2005) undertook water dialyses analysis using particles collected in Kumamoto (32° 48′N, 130° 45′E) in southwestern Japan. Their results indicated that 88% to 95% of dust aerosols were mixed with sea salt and that the post-dialysis number–size distributions of mineral and sea salt particles shifted toward smaller ranges compared to their pre-dialysis distribution. They concluded that the interaction of dust aerosols and sea salt is a likely and important process in size and composition changes of dust aerosols during their long-range transport.

Both results indicated that, in East Asia, the mixture of dust aerosols with sea salt and/or anthropogenic particles will commonly take place during their long-range transportation from source region to Japan.

3.4. Optical properties of dust

A large fraction of the RF attributed to dust depends on the dust optical thickness, asymmetry factor, and single scattering albedo (SSA). Among them, SSA is a primary factor in determining whether RF by aerosol species is positive or negative among the parameters of optical properties (e.g. Hansen et al., 1997; Nakajima et al., 2003). However, optical properties of mineral dust (MD) from Chinese deserts are not well understood and many uncertainties lie in the quantitative assessments of radiative effects due to dust. A considerable amount of work was conducted during the ACE-Asia campaign (Alfaro et al., 2003; Anderson et al., 2003; Murayama et al., 2003; Sano et al., 2003; Clarke et al., 2004). ACE-Asia was mainly conducted downwind of potential dust areas, in a coastal region and over the East China Sea. ADEC has been focusing on the dust emission processes in the source region and downwind areas in China and Japan. As depicted in Fig. 2, three sky-radiometers were operated in the dust source region (Aksu, Qira, and Shapotou in China), two in a downwind area in China (Beijing and Qingdao), and four in Japan (Naha, Fukuoka, Nagoya, and Tsukuba) (Uchiyama et al., 2005b).

It is known that ground-based sky radiometers can provide information that is inverted to yield column size distributions (Huebert et al., 2003). ADEC's sky-radiometer observation network was operated to evaluate the dust aerosol size change along with the long-range transport by measuring the effective radius r_{eff} at each site. The data analysis during IOP1 in April 2002 revealed four major results (Uchiyama et al., 2005b): (1) The contribution of the particles with radii greater than 0.5 μm, which corresponds to coarse dust particles, to the total optical thickness frequently exceeds 70% in the source region, Qingdao, and at Japanese sites on the dust event day. (2) The contribution of particles with radius greater than 0.5 μm to the total volume exceeds 80% on the dust event day at all sites. (3) The retrieved volume spectrum in the source region, Aksu and Qira, is not dependent on the optical thickness. This means that the floating aerosols mainly consist of dust particles in the source region. (4) When the size distribution for the coarse mode ($r > 0.5$ μm) is approximated by a lognormal size distribution, the effective radius r_{eff} is 2.1 to 2.3 μm at Chinese sites, and 1.6 to 1.8 μm at Japanese sites. The value r_g, where the logarithm of r_g is defined by the center of lognormal size distribution, is about 0.7 μm, at Aksu, Qira, and Shapotou and about 0.5 μm at other sites.

In addition to the optical parameters, which affect dust's RF, spectral albedo and reflectance of desert surface are important parameters for the Earth's radiation budget (Liao and Seinfeld, 1998). Aoki et al. (2005c) conducted a field measurement of spectral albedo and nadir reflectance of desert surfaces with a spectrometer for spectral region from 0.35 to 2.5 μm in western and central China in spring 2001 and fall 2003. The measured spectral albedos were low (0.05 to 0.11) at ultraviolet wavelengths but rapidly increased to 0.2 to 0.3 at about $\lambda = 0.6$ μm wavelength at all sites. The wavelength at which the albedo reached the maximum was around $\lambda = 1.8$ to 2.2 μm, where the albedos ranged from 0.37 to 0.49. Nadir reflectance exhibited a similar spectral distribution, while the values were lower than albedos at all wavelengths. Using these results, a retrieval method for Asian dust over land using ADEOS II/GLI data was subsequently proposed (Kuji et al., 2005).

Based on the ADEC data, sensitivity experiments of direct RF caused by MD for the optical and physical properties of MD were conducted using one dimensional radiative transfer model, the Streamer-based Radiative Transfer Model for ADEC Sciences (SARTMAS)

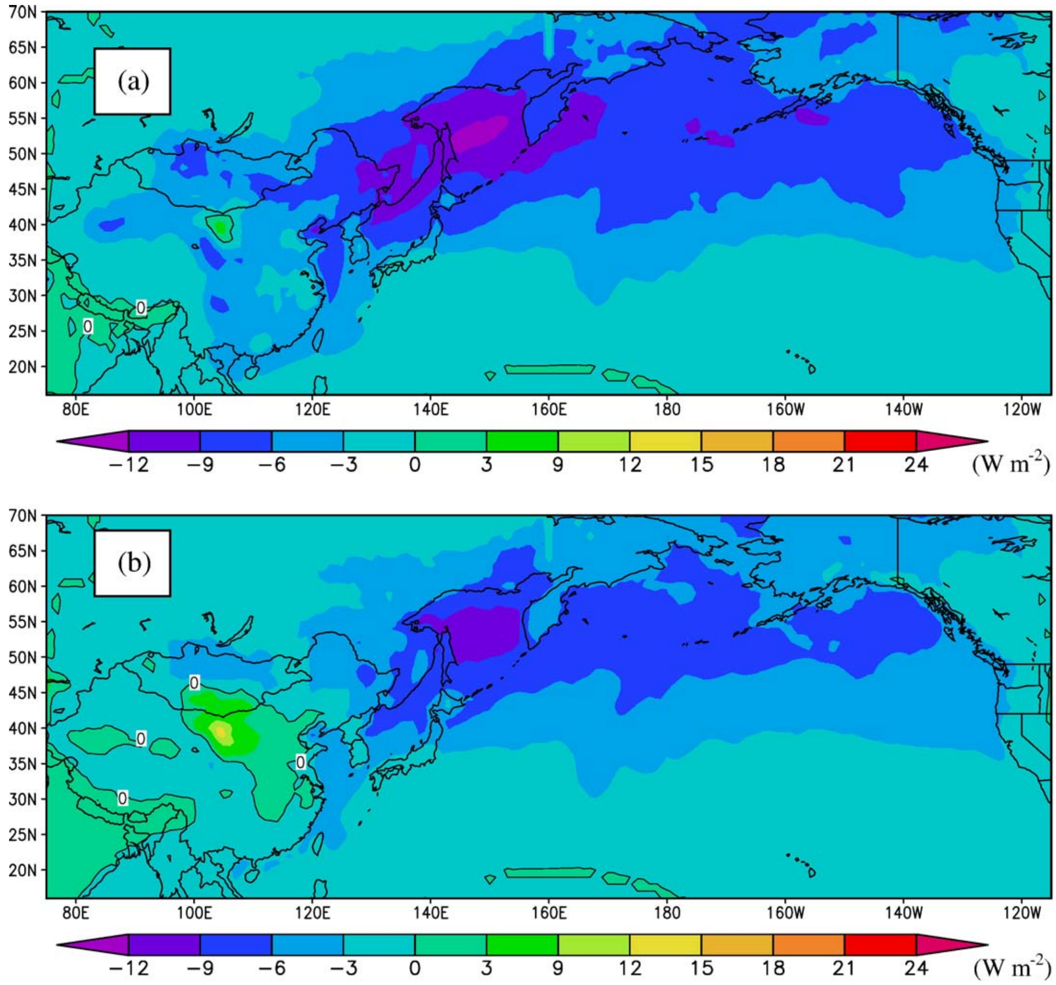

Fig. 20. Top of the Atmosphere radiative forcing (W m^{-2}) due to dust aerosol derived from data set of refractive indices of (a) ADEC-2 (Aoki et al., 2005b) and (b) Woodward (2001) dust models (modified from Shi et al., 2005 with permission from Meteorological Society of Japan).

(Aoki et al., 2005b) and using a *k*-distribution model for solar and thermal radiation transfer (Shi et al., 2005).

Aoki et al. (2005b) simulated the atmospheric and dust profiles with a chemical transport model MASINGAR (Tanaka et al., 2005) at four locations: the Sea of Japan, the desert in Tarim Basin, the Sahara Desert, and snow in Siberia. The experiment results confirmed that the sensitivity of instantaneous RF in the shortwave (SW) region at the top of the atmosphere (TOA) to the refractive index strongly depends on surface albedo. Namely, the effect of the difference in the MD model on instantaneous RF is significant over high albedo surfaces and is relatively small over the sea because the multiple reflections between the atmosphere (dust) and surface enhance light absorption by dust particles over high albedo surfaces. Over desert surfaces, the instantaneous RF in SW at TOA produced both positive and negative values within the possible refractive index range of MD. The diurnally averaged RF in SW at TOA also produced both positive and negative values in the possible range of desert albedo. It was found that for small dust particles with an effective radius of less than 0.6 μm, RFs by MD changed depending on the difference in surface type even if the broadband albedo was the same. The vertical positional relationship of cloud cover to dust layer was also very important for RF at TOA in all spectral regions over desert and sea surfaces. However, the effect of cloud cover was generally small over snow surface because cloud albedo was close to the underlying snow albedo.

Shi et al. (2005) performed numerical sensitivity experiments to evaluate the impact of optical

[1] This data source is incorrectly described as World Meteorology Organization (WMO) model in Shi et al. (2005).

Table 2
Comparison of global and annual mean dust budget for this study and recent studies of global dust model

	Emission ($Tg\ yr^{-1}$)	Dry deposition ($Tg\ yr^{-1}$)	Wet deposition ($Tg\ yr^{-1}$)	Dry/wet ratio	Load (Tg)	Lifetime (days)	Diameter range (μm)	Number of bins
This study	2149	1342	808	1.66	18.0	3.1	0.2–20	10
Mahowald et al. (1999)	3000	1840*	1170*	1.57	35*	4.3	Mass median	2.5, 1 bin
Takemura et al. (2000)	3321	2670	651	4.10	13.8	1.5	0.2–20	10
Ginoux et al. (2001)	1814	1606	235	6.83	35.9	7.2	0.2–12	7
Chin et al. (2002)	1650	1483	183	8.10	28.7	6.3	0.2–12	7
Tegen et al. (2002)	1100	724	374	1.94	22.2	7.4	0.2–440	7
Werner et al. (2002)	1060	811	244	3.32	8	2.8	0.2–438	7
Zender et al. (2003)	1490	866	607	1.43	17.4	4.3	0.1–10	4
Luo et al. (2003)	1654	823	798	1.03	23	5.1	0.1–10	4
Miller et al. (2004)	1019	595*	414*	1.44	14.6	5.2	0.2–16	4

characteristics on the RF. The experiments involved the effects of refractive indices, SSA, asymmetry factor and optical depth of MD. They used an updated data set of refractive indices of ADEC-2 model in Aoki et al. (2005b), which represents East Asian dust, and the data set by Woodward (2001).[1] The main differences between the two optical models are: (1) the real part of refractive index of the ADEC-2 model is slightly larger than that of the Woodward model (Woodward, 2001) at most wavelengths from solar to infrared bands; and (2) the imaginary part of refractive index of the ADEC-2 model is generally smaller than that of the Woodward model over solar wavelengths. Shi et al. used a *k*-distribution model (Shi, 1998) to calculate RF. Numerical simulation was conducted using the large dust event on 4 to 15 April 2001. The daily dust concentration was provided by the NARCM model by Gong et al. (2003). Their results indicate that the ADEC-2 model has stronger scattering and weaker absorption, which leads to higher negative forcing at the top of the atmosphere (TOA) as compared with the Woodward model (Fig. 20).

3.5. Modeling of global distribution of aeolian dust

A global-scale dust model is indispensable for evaluating dust's direct radiative effect on the global climate. The Model of Aerosol Species in the Global Atmosphere (MASINGAR) was developed for this purpose (Tanaka et al., 2003; Tanaka and Chiba, 2005). The model's dust emission processes are based on the saltation-bombardment theory (Owen, 1964; Shao et al., 1996; Shao, 2000), which expresses a size range of 10 bins from 0.2 to 20 μm in diameter. Erodibility factors for vegetation cover, snow cover, land use type, and soil type are considered. Dry and wet deposition processes are dependent on particle size. The model resolution is tunable from T21 (5.6×5.6°) to T106 (1.1×1.1°). Twenty-five years (from 1979 to 2003) were simulated using the T63 version (1.8×1.8°), and climatological global dust emission, deposition, and spatial distribution of dust aerosol were evaluated.

The simulated annual mean global emission flux and atmospheric dust load was evaluated to be 2149 $Tg\ yr^{-1}$ and 17.9 Tg in the size range $0.2 \le D \le 20$ μm. Dust-emission flux peaked around 7 μm. Emission flux of silt particles (1733 $Tg\ yr^{-1}$) was more than four times larger than that of clay particles (416 $Tg\ yr^{-1}$), but atmospheric burden of silt particles (8.0 Tg) was smaller than that of clay particles (10.0 Tg). The calculated emissions were within the range of recent model estimations (Table 2). Zonal mean dust distributions (Fig. 21) suggested that the dust from Asia and Africa travels at different altitudes, and that the Asian dust reaches a higher altitude (as high as 200 hPa) than the dust originating from other source regions.

3.6. Climate impact due to dust

Evaluation of RF due to the direct effect by dust aerosols is a goal for ADEC. Takahashi et al. (personal communication) evaluated RF due to the direct effect by dust aerosols using the global-scale dust model (MASINGAR). The optical properties of dust aerosols were based on OPAC (Hess et al., 1998) and simulation was conducted from 1998 to 2002 (five years). The simulated annual mean global emission flux was 2891 $Tg\ yr^{-1}$ and the atmospheric dust load was 24.2 Tg. The global-mean RF direct effect (DRF) at the top (bottom) of the atmosphere was estimated to be $-0.46\ W\ m^{-2}$ ($-2.13\ W\ m^{-2}$). This simulation was made under cloudy conditions. On the other hand, the global-mean DRF at TOP without cloudy conditions was estimated to be $-0.86\ W\ m^{-2}$, which is almost twice as much as that with cloudy conditions.

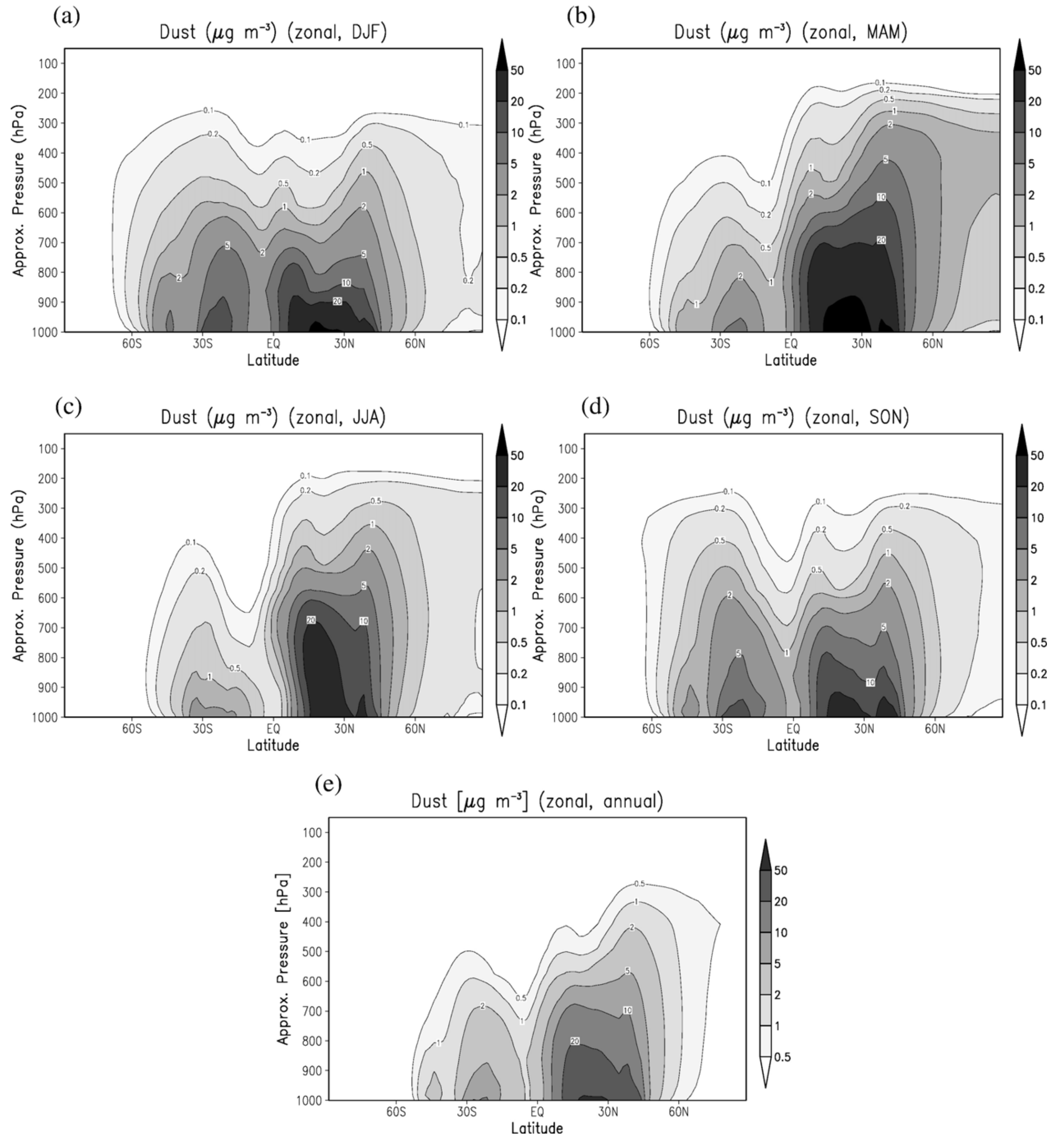

Fig. 21. Zonal mean dust concentration of dust aerosols by MASINGAR for (a) DJF, (b) MAM, (c) JJA, (d) SON, and (e) annual mean. Units are in μg m^{-3} (from Tanaka and Chiba, 2005 with permission from Meteorological Society of Japan).

Even if the global average of forcing is a considerably smaller value, heterogeneous atmospheric heating or cooling will yield regional differences in the temperature field of the stratosphere, which will result in changes in the atmospheric circulation. Atmospheric heating or cooling by direct effect of RF is thus important on a regional scale as well as on a global scale. Satake et al. (2004) simulated the radiative impact of Asian tropospheric aerosols, including dust, black carbon, organic carbon, and sea salt, using CFORS. Modeled aerosol optical thickness and Ångström exponent accurately captured many of the observed characteristics. Under overcast conditions, Asian dust has a large enough positive forcing to offset negative impacts of other aerosols due to the absorption of the radiation, which is enhanced by the cloud layer. The results of Satake et al. (2004) demonstrated that Asian-scale averaged direct RF due to dust aerosols at tropopause were -0.39 W m^{-2} for clear-sky condition and -0.16 W m^{-2} for all-sky condition, which indicate larger values than the annual global mean forcing by the GCM dust model result (Takemura et al., 2002).

During the ACE-Asia campaign in April 2001, aerosol radiative forcing using a three-dimensional aerosol transport-radiation model coupled with a

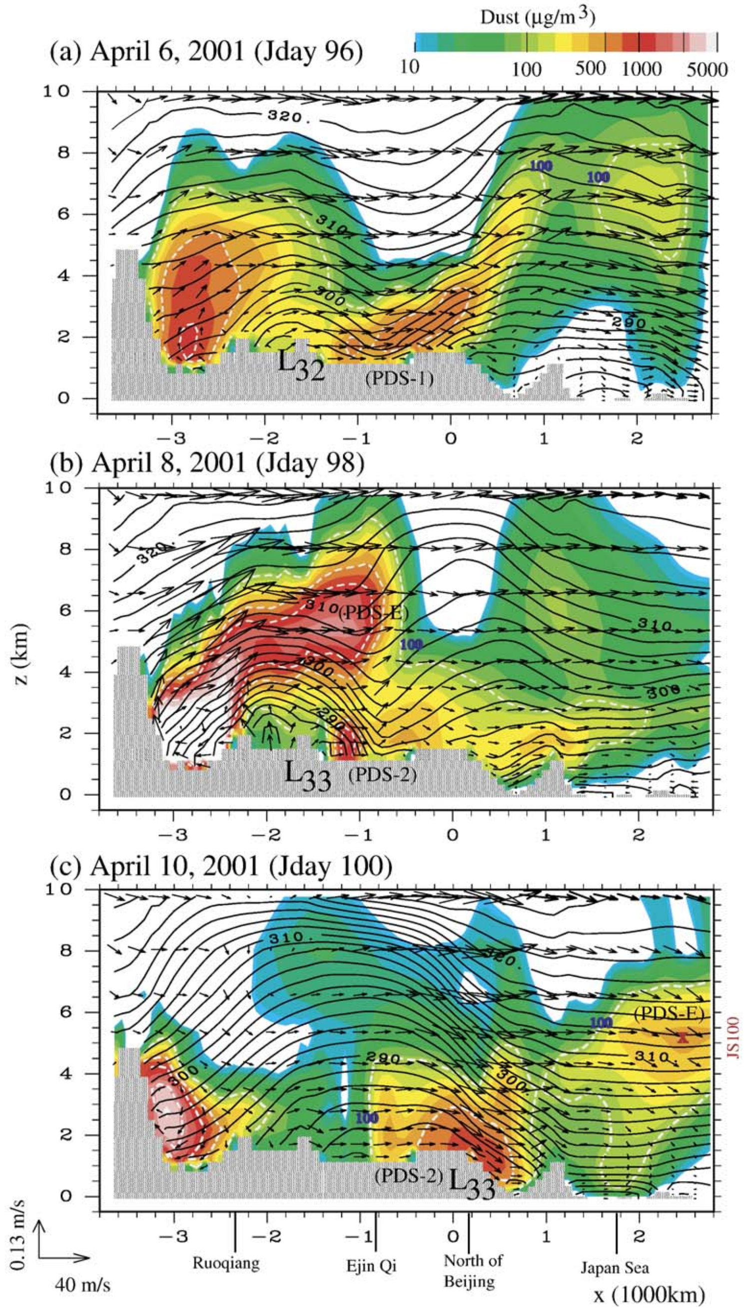

Fig. 22. (a–c) Vertical cross section of potential temperature (lines) and dust concentration (color) at selected west–east cross section line from the Taklimakan Desert to Japan at 0900 JST of each day. L32 and L33 comprise the low-pressure system. Vectors are u and w scaled as shown in wind scale (from Uno et al., 2004 with permission from American Geophysical Union).

general circulation model, SPRINTARS, was simulated as a part of the Asian Atmospheric Particulate Environmental Changes Studies (APEX) (Nakajima et al., 2003; Takemura et al., 2003). They simulated the direct effect of RF by the main tropospheric aerosols, that is, carbonaceous (organic carbon and black carbon), sulfate, sea salt, and soil dust in East Asia (90–152°E, 15–52°N). Their results indicate that the monthly and regional mean direct effect of RFs by dust are -0.19 W m^{-2} (TOA) and -1.07 W m^{-2} (Surface) under clear sky condition and are -0.02 W m^{-2} (TOA) and -0.93 W m^{-2} (Surface) under all-sky condition. Even though the horizontal scale and the period of the simulations are different among MASINGAR, CFORS, and SPRINTARS, their results are widely scattered. This is due to the fact that these dust models still have uncertainties, which include spatial distribution of dust in the troposphere, particle size distribution (Uno et al., in press), and optical properties, and absorption characteristics.

4. Discussion

4.1. Wind erosion process

The results from the Sand Particle Counter (SPC) clearly indicated that the number size distribution of the coarse particles ranging from 117 to 554 μm at 20 cm height exceeded that at 30 cm height; that is, streamwise mass flux q, which expresses the saltation of sand particles, is both height and particle size dependent (Mikami et al., 2005a). This variation of saltating particle size distribution with height is consistent with a previous result, which was observed in a cultivated paddock in Australia (Leys and Mctainsh, 1996). However, the present theory of saltation (e.g., Shao and Raupach, 1992; Gillette et al., 1997) does not explain these height dependencies of saltation particle number density. Recently, theoretical considerations have been made to establish a new similarity theory for the saltation process that can express the vertical profile of saltation flux $q(d)$ (Shao, 2005; Shao and Mikami, 2005). This similarity theory demonstrates that q decays exponentially with height for large particles saltating in weak turbulence; and that q is Gaussian for small particles saltating in strong turbulence. For multi-sized particles, q is a weighted average of many saltation mass flux profiles that differ for different particle sizes (Shao, 2005). Currently, only a few observations of the vertical profile of saltation flux q have been made, so the validation of this theory is still required with various soil types and ground surface conditions.

As with saltation flux, vertical flux of dust emission F is a function of height and dust particle size (Shao, 2000). The value F is generally expressed as a functional form of saltation flux. This scheme is commonly used for dust models. Dust model inter-comparison (DMIP) revealed a large difference among nine dust emission models (Xie et al., 2005). To improve model representation of dust flux, models must be validated against observations. However, measurement of vertical dust flux at high time resolution is very difficult due to the need to measure number concentration and particle size. In addition to monitoring saltation processes, ADEC focused on monitoring vertical dust flux in a source region. Using OPC, vertical profiles of dust particle number concentration from 0.3 to 7.5 μm were obtained with meteorological and soil physical conditions during IOP3 2004 (Mikami et al., 2004).

4.2. Multiple dust layer in East Asia and its indirect effect on radiative forcing

From the commencement of lidar observations in East Asia, a dust aerosol layer was identified in the free troposphere (Iwasaka et al., 1983). At Nagoya, central Japan, lidar observations during March to May 1994 also revealed a presence of weak dust layers from 2 to 6 km height (Matsuki et al., 2003). Uno et al. (2004) numerically simulated a huge dust event, referred to as the "Perfect Dust Storm," on April 2001 using his chemical transport model, CFORS. The model analysis showed that the dust loading is transported with the meandering of the synoptic-scale temperature field at the 500 hPa level. This dust storm consisted of two boundary layer components and one elevated dust layer in the free troposphere (≥6 km height). A sensitivity analysis indicated that the origin of the elevated dust layer was the Taklimakan Desert, whereas the lower dust layer in the boundary layer originated from the Gobi Desert. The model simulation revealed that, over the Taklimakan region, strong wind conditions and a weak potential temperature gradient resulted in the lifting of large amounts of dust (Fig. 22).

The global scale dust model (MASINGAR) also revealed the relative importance of elevated dust layer on cross-continental dust transport (Tanaka et al., 2005). From the evening of 25–27 March 2003, Kosa phenomena were reported in 37 routine meteorological observatories in Japan at a time when no significant dust storms had been observed in the arid regions of China or Mongolia. During this time, the Aksu lidar located in the Taklimakan Desert detected a dust layer in the troposphere (6 to 11 km) and lidar sites at Tsukuba (36.0°N, 140.1°E) and Naha (26.1°N, 127.4°E), in Japan, also detected a dust layer at 2 to 6 km. The MASINGAR simulation results indicated that the observed mineral dust was generated through dust storms in the Sahara Desert and the Arabian Peninsula on 19 March and was transported north of the Tien-Shan Mountains in China. According to the model, this dust arrived over Japan in the free troposphere (2 to 6 km) within six to seven days. The model result was consistent with the measurements by the ADEC polarization lidar (Tsunematsu et al., in press) and the sky-radiometer network (Uchiyama A., personal communication). MASINGAR simulated that over 50% of the dust particles in Japan on 26–27 March came from North Africa and 30% from the Middle East. This suggests that dust in the free troposphere can be transported on a cross-continental scale and, in some cases, dust from North Africa and the Middle East will be significant for the East Asia atmospheric environment.

During ADEC experiments, Raman lidar measurement demonstrated the importance of elevated dust layer in the free troposphere on the indirect effect of RF. Sakai et al. (2004) conducted a measurement of vertical distributions of particle extinction, backscattering, depolarization, and water vapor mixing ratio over Tsukuba (36.1 °N, 140.1°E), Japan. They found ice clouds associated with the Asian dust layer at an altitude of approximately 6 to 9 km. The relative humidity (estimated from lidar-derived water-vapor mixing ratio and the radiosonde-derived temperature and pressure profile) in the cloud layer was close to the ice saturation values and the temperature at the top of the cloud layer was approximately −35 °C, suggesting that the Asian dust acted as ice nuclei at higher temperatures. This ice-saturated region was formed near the top of the dust layer. These processes will generally occur in East Asia in a "background Kosa" environment (Murayama, 2001). Even at great transport distances from Asian dust source region, Sassen (2005) found a connection between transported Asian aerosols and icy dust clouds observed during spring 2004 over the interior of Alaska. These findings suggest that indirect effects of desert dust on cloud formation (Isono et al., 1959) and composition may be considerable.

On the other hand, a lower dust layer within the boundary layer (originating from the Gobi Desert (Uno et al., 2004)) is an important factor in the indirect effect of RF in East Asia. Asian dust sources are located in the inland area of China and they are mixed with anthropogenic particles that are emitted from highly

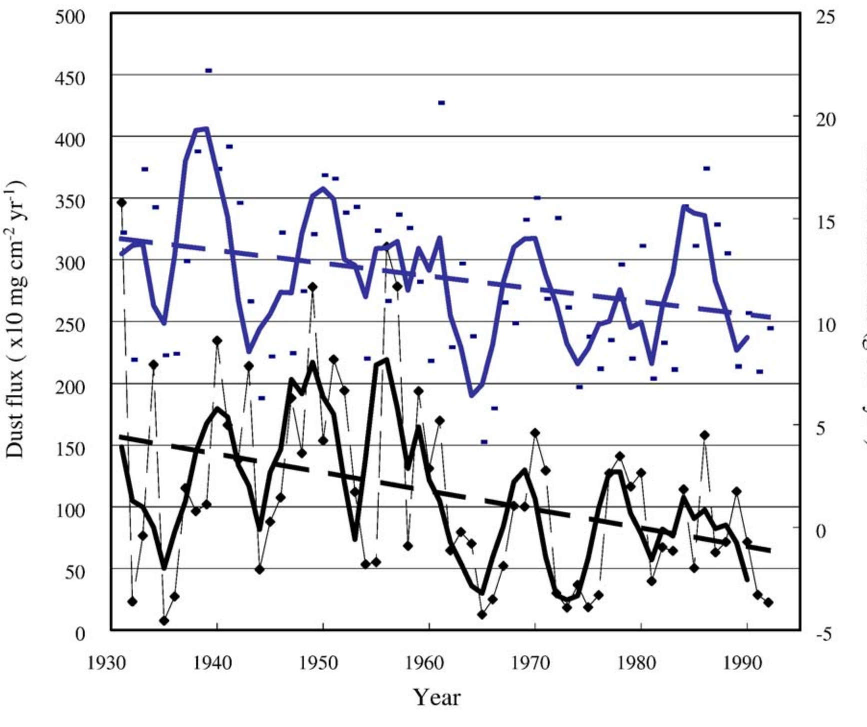

Fig. 23. Parallel variation of dust flux (lower set) an accumulation rate (upper set) in the 1930s to 1990s recorded in the Chongce ice core. The solid lines represent the three-year's smoothing average (from Han and Nakawo, 2005).

industrialized areas located in the downwind region. These dust/pollution mixtures are thought to be activated as cloud condensation nuclei, which are related to the indirect effect of RF.

4.3. Optical properties of dust

SSA is a primary factor in determining whether RF due to MD is positive or negative in the atmosphere (Aoki et al., 2005b). Recently, SSA for Saharan dust has been found to have a higher value (Kaufman et al., 2001; Haywood et al., 2001, 2003) than that previously reported (Shettle and Fenn, 1979, Hess et al., 1998, Sokolik and Golitsyn, 1993). However, data on SSA features in dust source regions in East Asia are lacking to date. ADEC research has tried to reveal the SSA features in East Asia from dust source regions to downwind area, Japan.

Uchiyama et al. (2005a) retrieved SSA from sky-radiometer data using the latest version of the Skyrad package (Nakajima et al., 1996) in the ADEC network sites from the Taklimakan Desert to Japan. The differences between actual and retrieved SSA are small when the total column optical thickness is estimated from the attenuation of the direct solar irradiance. Therefore, careful calibration of the sky-radiometer, against the well-calibrated sun-photometer at Mauna Loa Observatory was undertaken every year. The averaged SSAs during ADEC IOP1, April 2002, at Aksu, Qira, Shapatou, Qingdao, Naha, Fukuoka, Nagoya, and Tsukuba were 0.955, 0.933, 0.914, 0.942, 0.944, 0.953, 0.933, and 0.973, respectively. In addition to the retrieved SSA analysis, in situ measurements of SSA by Particle Soot Absorption Photometer (PSAP; Radiance Research) and Nephelometer (M903; Radiance Research) were carried out at Qira, Beijing, and Tsukuba (Uchiyama et al., 2005a). SSA measured by PSAP and M903 were between 0.91 and 0.93 at Qira, between 0.80 to 0.88 at Beijing, and between 0.8 and 0.9 at Tsukuba. The SSA measured by PSAP and M903 at Qira were consistent with the SSA inferred from the sky-radiometer. This means that unpolluted aeolian dust has lower absorption than originally believed. The SSA derived from PSAP and M903 at Beijing and Tsukuba is lower than the SSA inferred from the sky-radiometer. This is partly because the SSA derived from PSAP represents information of dust particles near the surface and, hence, represents the dust particles mixed with absorbing aerosols during long range transport within the boundary layer.

Both PSAP and Nephelometer have an error of 10% to 20% and tend to underestimate (Anderson et al., 1996; Bond et al., 1999). However, the resultant SSA error from both instruments is thought to be from 1% to 2%. This level of error is acceptable for qualitative discussion of SSA from source to downward region. For quantitative discussion, accurate calibration is required for PSAP and Nephelometer. But we do not have reliable calibration methods at present. The software used to retrieve SSA from sky-radiometer data assumes particles are spherical, although dust particles are generally non-spherical in shape.

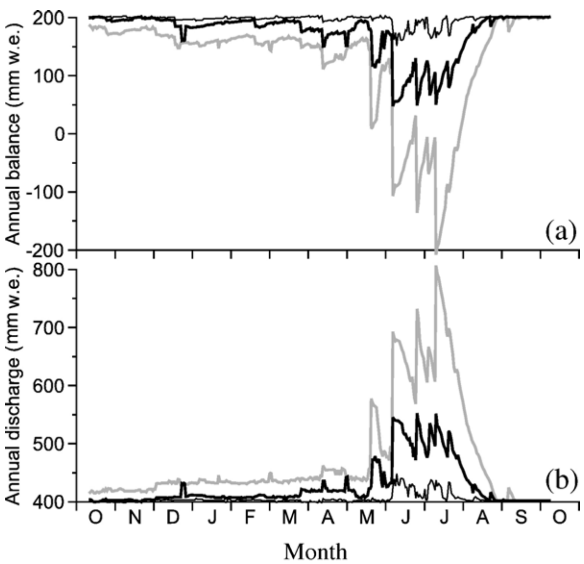

Fig. 24. Seasonal sensitivities of mass-balance (a) and discharge (b) on the changes in dust deposited date (unit in mm water equivalent; mm w.e.). Horizontal and vertical axes denote the date when dust was deposited, and the areal averaged annual balance (a) and discharge (b) at the end of calculation period. Albedo of the dusted is assumed to be 0.7 (thin lines), 0.6 (thick lines) and 0.58 (gray lines), respectively (modified from Fujita, 2002 with permission from the Japanese Association for Arid Land Studies).

4.4. Cryosphere and dust interaction

Motoyoshi et al. (2005) observed broadband snow albedos in the visible and near infrared spectral regions using the snow pit method over an interval of several days, during the winters of 2001/2002 and 2002/2003 at Shinjo, Japan. The comparisons between measured albedos and theoretical ones (calculated using a radiative transfer model for atmosphere–snow systems) revealed that the snow was contaminated by strong absorptive impurities such as soot, in addition to moderate absorptive impurities such as mineral dust.

Measurement of atmospheric aerosols above the snow surface using an OPC suggested that wet deposition of atmospheric aerosols caused snow impurities of more than 1 ppmw in mass concentration. When dust aerosol is deposited onto the snow surface, it reduces the visible albedo that will result in a climatic change in the cryosphere due to the change in the surface energy budget of the snow cover (Nakawo and Fujita, 2005; Aoki et al., 2005a; Motoyoshi et al., 2005).

Han and Nakawo (2005) reported the temporal variation of dust flux during the past 60 years using ice core samples drilled from an ice dome, 6530 m above sea level, in the Chongce Ice Cap in the West Kunlum Mountains. The temporal variation of dust flux indicates a clear correlation with the change in snow accumulation rate (Fig. 23). They suggested a close relationship between dust particles and snowfall through the precipitation forming process via activation of dust particle as an ice nucleus. This interactive process is an indirect impact of aeolian dust on the local climate and hydro water cycle in a cryosphere.

The effect of dust deposition onto glaciers is not well represented in the current glacier model, which aims to evaluate the water resources and cycle of inland river basin of the continents, such as central Asia. Only Fujita (2002) has tried to simulate the interaction of cryosphere and dust in his glacier mass balance model that was applied to reveal the impact of dust on glacier mass balance of the Tibetan Plateau. Fig. 24 shows the seasonal sensitivities of mass balance (a) and discharge (b) on the changes in the dust deposition date assuming low albedo of dusted surface. The dust depositions in June and July reduce the annual mass balance by < -100 mm (water equivalent) and increase the discharge by 40% (albedo = 0.6) due to the absorption of intense solar radiation in this season. The impact of dust deposition is remarkably greater than those of changes in the meteorological variables (Fujita and Ageta, 2000). It should be noted that such a large negative/positive impact on glacier mass-balance/discharge would be caused even if dust was deposited in only one day during June and July.

4.5. Dust Model Intercomparison Project: DMIP

Many dust models are now used for forecasting dust and sand storms and for climate research. There has been no systematic comparison of regional or global scale dust models. For this reason, ADEC organized a dust model inter-comparison (DMIP) (Uno et al.,http://cfors.riam.kyushu-u.ac.jp/~cfors/DMIP/). Nine models from six countries were used to simulate two typical dust episodes, 15 to 25 March 2002 and 4 to 14 April 2002. Dust emission fluxes were compared within the region of 35° to 50°N and 75° to 125°E. Comparisons were undertaken for dust production mechanism, threshold friction velocity, mean dust emission flux from selected period, snap friction velocity, and dust flux for a specified time.

Results reveal that a large discrepancy in threshold friction speed, friction velocity and functions for calculating dust emission flux can be found. These discrepancies will come from the differences in meteorological models, mechanism of dust production, and soil condition (Uno et al., in press). Although the comparison was limited to two cases, more work is expected in the future.

4.6. Future research issues beyond ADEC

Although a great deal of research was undertaken during ADEC, many questions remain to be answered.

i) ADEC has been focusing on dust emission from the natural ground surface in arid regions. Anthropogenic dust emission is, however, a concern for assessing climate impact due to dust aerosols (IPCC, 2001). Quantification of anthropogenically disturbed dust caused by over grazing and inappropriate cultivation of land and/or water management in semi-arid regions is required.
ii) While monitoring of dust over oceans has been achieved using GMS-5 (Masuda et al., 2002, 2003, 2005) during ADEC experiments, in order to monitor the horizontal distribution of dust and to validate the dust model, horizontal information of dust over land is required. A retrieval technique using satellite data is still in the development stage (e.g. Gu et al., 2003; Kuji et al., 2005).
iii) In many East Asian countries, the need is very high for an operational dust model for predicting dust storms and TSP, PM2.5, and PM10 concentrations. DMIP revealed that the present dust models have a large discrepancy in the temporal and spatial representation of dust. For improving model representation of dust distribution and its long-distance transportation, verification of model results with observation and development of data assimilation techniques for retrieving lidar and dust sampling information are necessary. As for the model evaluation of direct effect of RF due to dust, there still remain uncertainties especially for optical properties of dust particle.
iv) The dust storm outbreak frequency (DOF) variation is generally consistent with the strong

wind frequency (SWF) in East Asia; however, it is not clear why this SWF variability occurs. Some modeling investigations suggested a relation to the Arctic oscillation (AO) (Hara et al., 2004). Atmospheric dust loading and large-scale atmospheric circulation may be inter-related to each other through heterogeneous atmospheric heating/cooling by dust aerosols. In addition, DOF is related to ground surface conditions such as snow cover, vegetation, and soil wetness (Kurosaki and Mikami, 2004). These ground surface conditions are also related to be inter-annual variation of large-scale atmospheric circulation systems. Therefore, the relationship between dust and climate is a highly complex and interactive process as illustrated in Fig. 1.

5. Summary and conclusions

The Aeolian Dust Experiment on Climate Impact (ADEC) was initiated in April 2000 as a five-year joint Japan–China project. The goal of this project was to understand the impact of aeolian dust on the climate system via RF. We conducted field experiments and numerical simulations to understand the following processes: (1) wind erosion, (2) dust concentration, vertical distribution, and deposition, (3) characterization of aeolian dust: physical, chemical, and optical properties, and (4) climatic impact of aeolian dust via RF direct effect. We established an observation network of 10 sites from the Taklimakan Desert source region to Japan and undertook intensive observations, during April 2002 (IOP1), March 2003 (IOP2), and March to April 2004 (IOP3). Our achievements are summarized as follows:

It is clear from in situ observation of dust outbreak process at source region that saltation is a complex process, which depends on height, particle size, and soil wetness, and the recent theory of saltation needs to be improved to explain this.

Lidar measurements observed multiple dust layers in the free troposphere over East Asia. These multiple dust layers were also represented by a numerical simulation of the “Perfect Dust Storm” on April 2001 using CFORS. CFORS also clearly illustrated the multiple dust layers in East Asia: one in the free troposphere originated from the Taklimakan Desert and the other in the boundary layer originated from the Gobi Desert.

The global-scale dust model, MASINGAR, simulated the presence of dust layer at the middle to upper troposphere during the dust event in March 2003, which originated from dust storms in North Africa and the Middle East. The ice clouds associated with the Asian dust layer at altitudes of 6 to 9 km were observed at Tsukuba using the Raman lidar. Analysis from Raman lidar and the radio-sonde observation suggested that the Asian dust acted as ice nuclei forming near the top of the dust layer in ice-saturated regions. Thus, the presence of multiple dust layers in East Asia implies the dust’s climate impact in two different ways: the first is that the dust transported in the free troposphere will be activated as ice nuclei, which is an indirect effect of RF due to dust. The second is that the dust in the boundary layer in East Asia will internally and/or externally mixed with anthropogenic aerosols and with sea salt during its long-range transportation and will impact on another indirect effect of RF via activation of dust particles as a CCN.

RF by MD was directly evaluated using the global-scale dust model. The simulated global mean direct RF was estimated to be -0.46 W m^{-2} at TOA and -2.13 W m^{-2} at the bottom with cloudy condition. Sensitivity experiments of direct RF by MD indicated that SSA is a primary factor for direct RF by MD whether it is positive or negative and that the sensitivity of instantaneous RF in the shortwave region at TOA to the refractive index is strongly dependent on surface albedo. Over desert and sea surfaces, the vertical positional relationship of cloud cover to the dust layer is also very important for RF of TOA in all spectral regions.

Generally, we were successful in understanding East Asian dust characterization and its outbreak and transport processes. Through three intensive observation periods at network sites using lidar, sky-radiometer, and aerosol samplers, we have begun to understand the long-range transport processes of dust and its physical, chemical, and optical properties from source region to downwind area. The in situ observation of dust outbreak process at the source region has successfully described the saltation process. As a result, a new saltation theory is required.

The global dust model, MASINGAR, was used to evaluate the direct effect of RF due to dust. The result implies that the global mean forcing is comparatively small but its regional impact is significant, especially in East Asia. It is clear, however, that large uncertainties still remain in the quantitative measurement, mainly due to uncertainties with optical properties of dust and model representation. Linkages between dust and local and/or global climate are suggested through ice core analysis and an integrated analysis of network observations and regional dust model simulations. These linkages are not confirmed by the data at present, so future experiments are required to reveal these processes.

The ADEC was the first comprehensive program of dust research in East Asia. These findings have shown that there is successive research still to be undertaken to improve our understanding of dust's impact on climate.

Acknowledgement

The ADEC experiment is sponsored by the Ministry of Education, Culture, Sports, Science and Technology, the Japanese government and by the Chinese Academy of Sciences. This study is supported by JSPS. KAKENHI (17201008).

References

Alfaro, S.C., Gomes, L., Rajot, J.L., Lafon, S., Gaudichet, A., Chatenet, B., Maille, M., Cautenet, G., Lasserre, F., Cachier, H., Zhang, X.Y., 2003. Chemical and optical characterization of aerosols measured in spring 2002 at the ACE-Asia supersite, Zhenbeitai, China. J. Geophys. Res. 108 (D23), 8641. doi:10.1029/2002JD003214.

Anderson, T.L., Covert, D.S., Marxhall, S.F., Laucks, M.L., Charlson, R.J., Waggoner, A.P., Ogren, J.A., Caldow, R., Holm, R.L., Quant, F.R., Sem, G.J., Wiedensohler, A., Ahlquist, N.A., Bates, T.S., 1996. Performance characteristics of a high-sensitivity, three-wavelength, total scatter/backscatter nephelometer. J. Atmos. Ocean. Technol. 13, 967–986.

Anderson, T.L., Masonis, S.J., Covert, D.S., Ahlquist, N.C., Howell, S.G., Clarke, A.D., McNaughton, C.S., 2003. Variability of aerosol optical properties derived from in situ aircraft measurements during ACE-Asia. J. Geophys. Res. 108 (D23), 8647. doi:10.1029/2002JD003247.

Aoki, T., Motoyosi, H., Kodama, Y., Yasunari, T.J., Kobayasi, H., Uchiyama, A., Chiba, M., Tanaka, T.Y., 2005a. Atmospheric aerosol deposition on snow surface and its effect on albedo. Proc. Fourth ADEC 317–320.

Aoki, T., Tanaka, T.Y., Uchiyama, A., Chiba, M., Mikami, M., Yabuki, S., Key, J., 2005b. Sensitivity experiments of direct radiative forcing by mineral dust using spectrally detailed radiative transfer model. J. Meteorol. Soc. Jpn. 83A, 315–331.

Aoki, T., Mikami, M., Yamazaki, A., Yabuki, S., Yamada, Y., Ishizuka, M., Zeng, F.-J., Gao, W.-D., Sun, J.-Y., Liu, L.-C., Zhou, M.-X., 2005c. Spectral albedo of desert surface measured in Western and Central China. J. Meteorol. Soc. Jpn. 83A, 279–290.

Bond, T.C., Anderson, T.L., Campbel, D., 1999. Calibration and intercomparison of filter-based measurements of visible light absorption by aerosols. Aerosol Sci. Technol. 30, 582–600.

Bory, A.J.-M., Biscaye, P.E., Grousset, F.E., 2003. Two distinct seasonal Asian source regions for mineral dust deposited in Greenland (NorthGRIP). Geophys. Res. Lett. 30 (4), 1167. doi:10.1029/2002GL016446.

Chin, M., Ginoux, P., Kinne, S., Torres, O., Holben, B.N., Duncan, B.N., Martin, R.V., Logan, J.A., Higurashi, A., Nakajima, T., 2002. Tropospheric aerosol optical thickness from the GOCART model and comparisons with satellite and sun photometer measurements. J. Atmos. Sci. 59, 461–483.

Clarke, A.D., Shinozuka, Y., Kapustin, V.N., Howell, S., Huebert, B., Doherty, S., Anderson, T., Covert, D., Anderson, J., Hua, X., Moore II, K.G., McNaughton, C., Carmichael, G., Weber, R., 2004. Size distributions and mixtures of dust and black carbon aerosol in Asian outflow: physiochemistry and optical properties. J. Geophys. Res. 109. doi:10.1029/2003JD004378 (D15S09).

Dayan, U., Heffler, J., Miller, J., Gutnan, G., 1991. Dust intrusion events into Mediterranean Basin. J. Appl. Meteorol. 30, 1185–1199.

Ding, R., Li, J., Wang, S., 2005. Decadal change of the spring dust storm in northwest China and the associated atmospheric circulation. Geophys. Res. Lett. 32. doi:10.1029/2004GRL21561 (L02808).

Du, M., 2002. Wind erosion processes during dust storm in Dunhuang, China. Proc. 12th ISCO 624–629.

Duce, R.A., Uni, C.K., Ray, B.J., Prospero, J.M., Merrill, J.T., 1980. Long-range atmospheric transport of soil dust from Asia to the tropical North Pacific: temporal variability. Science 209, 1522–1524.

Duce, R.A., Liss, C.K., Merrill, J.T., Atlsa, E.L., Buat-Menard, P., Hucks, B.B., Miller, J.M., Prospero, J.M., Arimoto, R., Church, T. M., Ellis, W., Galloway, J.N., Hansen, L., Jickells, T.D., Knap, A. H., Reinhardt, K.H., 1991. The atmospheric input of trace species to the world ocean. Glob. Biogeochem. Cycles 5, 193–259.

Fe´can, F., Marticorena, B., Bergametti, G., 1999. Parameterization of the increase of the aeolian erosion threshold wind friction velocity due to soil moisture for arid and semi-arid areas. Ann. Geophys. 17, 149–157.

Fujita, K., 2002. Impact of dust on glacier mass balance of the Tibetan Plateau. J. Arid Land Stud. 11, 355–360.

Fujita, K., Ageta, Y., 2000. Effect of summer accumulation on glacier mass balance on the Tibetan Plateau revealed by mass-balance model. J. Glaciol. 46 (153), 244–252.

Gillette, D.A., Fryrear, D.W., Xiao, J.B., Stockton, P., Ono, D., Helm, P.J., Gill, T.E., Ley, T., 1997. Large-scale variability of wind erosion mass flux rates at Owens Lake 1. Vertical profiles of horizontal mass fluxes of wind-eroded particles with diameter greater than 50 μm. J. Geophys. Res. 102 (D22), 25977–25987.

Ginoux, P., Chin, M., Tegen, I., Prospero, J.M., Holben, B., Dubovik, O., Lin, S.-J., 2001. Sources and distributions of dust aerosols simulated with the GOCART model. J. Geophys. Res. 106, 20255–20273.

Gong, S.I., Zhang, X.Y., Zhao, T.I., Mckendry, I.G., Jaffe, D.A., Lu, N.M., 2003. Characterization of soil dust aerosol in China and its transport and distribution during 2001 ACE-Asia: 2. Model simulation and validation. J. Geophys. Res. 109 (D9). doi:10.1029/2002JD002633.

Gu, Y., Rose, W.I., Bluth, G.I.S., 2003. Retrieval of mass and sizes of particles in sandstorms using two MODIS IR bands: a case study of April 7, 2001 sandstorm in China. Geophys. Res. Lett. 30. doi:10.1029/2003GL017405.

Han, J., Nakawo, M., 2005. Ice core record in an Asian glacier of 6350 m a.s.l.: overall declination of atmospheric dust flux for past 60 a. Proc. Fourth ADEC 313–316.

Hansen, J., Sato, M., Ruedy, R., 1997. Radiative forcing and climate response. J. Geophys. Res. 102 (D6), 6831–6864.

Hara, Y., Satake, S., Uno, I., Takemura, T., 2004. Interannual Variations of 'Kosa' Simulated by a Regional-Scale Dust Transport Model. Tenki 51, 719–728 (in Japanese).

Hayashi, M., Yamashita, K., Ozuka, K., Shiraishi, K., Otobe, N., Yamamoto, T., Chen, B., Shi, G., 2005. Variation of size distribution and mineral composition of aeolian dust in the boundary layer at Hun Huang, China: unmanned airplane measurement in spring and summer from 2002 to 2004. Proc. Fourth ADEC Workshop 247–250.

Haywood, J.M., Francis, P.N., Glew, M.D., Taylor, J.P., 2001. Optical properties and direct radiative effect of Saharan dust: a case study of two Saharan dust outbreaks using aircraft data. J. Geophys. Res. 106, 18417–18430. doi:10.1029/2000JD900319.

Haywood, J., Francis, P., Osborne, S., Glew, M., Loeb, N., Highwood, E., Tanré, D., Myhre, G., Formenti, P., Hirst, E., 2003. Radiative properties and direct radiative effect of Saharan dust measured by the C-130 aircraft during SHADE: 1. Solar spectrum. J. Geophys. Res. 108, 8577. doi:10.1029/2002JD002687.

Hess, H., Koepke, P., Schult, I., 1998. Optical properties of aerosols and clouds: the software package OPAC. Bull. Am. Meteorol. Soc. 79, 831–844.

Huebert, B.J., Bates, T., Russell, P.B., Shi, G., Kim, Y.J., Kawamura, K., Carmichael, G., Nakajima, T., 2003. An overview of ACE-Asia: strategies for quantifying the relationships between Asian aerosols and their climatic impacts. J. Geophys. Res. 108 (D23), 8633. doi:10.1029/2003JD003550.

Intergovernmental Panel on Climate Change (IPCC), 2001. In: Houghton, J.T., et al. (Ed.), Climate Change 2001, The Scientific Basis. Cambridge Univ. Press, New York.

Ishizuka, M., Mikami, M., Yamada, Y., Zeng, F., Gao, W., 2005. An observational study of soil moisture effects on wind erosion at a gobi site in the Taklimakan Desert. J. Geophys. Res. 110. doi:10.1029/2004JD004709 (D18S03).

Isono, K., Komabayashi, M., Ono, A., 1959. The nature and the origin of ice nuclei in the atmosphere. J. Meteorol. Soc. Jpn. 37, 211–233.

Iwasaka, Y., Minoura, H., Nagaya, K., 1983. The transport of spatial scale of Asian dust-storm clouds: a case study of the dust-storm event of April 1979. Tellus 35B, 189–196.

Iwasaka, Y., Shibata, T., Nagatani, T., Shi, G.-Y., Kim, Y., Matsuki, S., Trochikine, A., Zhang, D., Yamada, D., Nagatani, M., Nakata, M., Xhen, H., Li, Z., Chen, G., Kawahira, B., 2003a. Large depolarization ratio of free tropospheric aerosols over the Taklimakan Desert revealed by lidar measurements: possible diffusion and transport of dust particles. J. Geophys. Res. 108 (D23), 8652. doi:10.1029/2002JD003267.

Iwasaka, Y., Shi, G.-Y., Yamada, M., Matsuki, A., Trochkine, D., Kin, Y.S., Zhang, D., Nagatani, T., Shibata, T., Nagatani, M., Nakata, H., Shen, Z., Li, G., Chen, B., 2003b. Importance of dust particles in the free troposphere over the Taklimakan Desert: electron microscopic experiments of particles collected with a balloonborne particle impactor at Dunhuang, China. J. Geophys. Res. 108 (D23). doi:10.1029/2002JD003270.

Kai, K., Tsunematsu, N., Goto, M., Matsumoto, T., Hongfei, Z., Shunjun, H., Abo, M., Nagai, T., Matsumura, T., 2005. Summary of the Aksu Lidar Observations during 2002–2004 — structure of the dust layer over the Taklimakan Desert. Proc. Fourth ADEC Workshop 187–190.

Kanai, H., Ohta, A., Kamioka, H., Terashima, S., Imai, N., Kanai, M., Shimizu, H., Takahashi, Y., Kai, K., Hayashi, M., Zhang, R., Sheng, L., 2005. Long-term trend and characterization of aeolian dust in east China and Japan from 2001 to 2003. J. Meteorol. Soc. Jpn. 83A, 73–106.

Kanayama, S., Yabuki, S., Zeng, F., Liu, M., Shen, Z., Liu, L., Yanagisawa, F., Abe, O., 2005. Size-dependent geochemical characteristics of Asian dust — Sr and Nd isotope compositions as tracers for source identification. J. Meteorol. Soc. Jpn. 83A, 107–120.

Kaufman, Y.J., Tanré, D., Dubovik, O., Karnieli, A., Remer, L.A., 2001. Absorption of sunlight by dust as inferred from satellite and ground-based remote sensing. Geophys. Res. Lett. 28, 1479–1482.

Kuji, M., Yamada, N., Hayashida, S., Yasui, M., Uchiyama, A., Yamazaki, A., Aoki, Te., 2005. Retrieval of Asian dust amount over land using ADEOS-II/GLI near UV data. SOLA 1, 33–36.

Kurosaki, Y., Mikami, M., 2003. Recent frequent dust events and their relation to surface wind in east Asia. Geophys. Res. Lett. 30 (14), 1736. doi:10.1029/2003GL017261.

Kurosaki, Y., Mikami, M., 2004. Effect of snow cover on threshold wind velocity of dust outbreak. Geophys. Res. Lett. 31. doi:10.1029/2003GL018632 (L03106).

Lee, S.-S., Chun, Y., Nam, J.-C., Park, S.-U., Lee, E.-H., 2005. Estimation of dry deposition during Asian dust events in Spring of 2002. J. Meteorol. Soc. Jpn. 83A, 241–254.

Leys, J., Mctainsh, G., 1996. Sediment fluxes and particle grain-size characteristics of wind-eroded sediments in southeastern Australia. Earth Surf. Process. Landf. 21, 661–671.

Liao, H., Seinfeld, J.H., 1998. Radiative forcing by mineral dust aerosols: sensitivity to key variables. J. Geophys. Res. 103, 31637–31645.

Luo, C., Mahowald, N.M., del Corral, J., 2003. Sensitivity study of meteorological parameters on mineral aerosol mobilization, transport, and distribution. J. Geophys. Res. 108 (D15), 4447. doi:10.1029/2003JD003483.

Mahowald, N., Kohfeld, K., Hansson, M., Balkanski, Y., Harrison, S.P., Prentice, I.C., Schulz, M., Rodhe, H., 1999. Dust sources and deposition during the last glacial maximum and current climate: a comparison of model results with paleodata from ice cores and marine sediments. J. Geophys. Res. 104, 15895–15916.

Masuda, K., Mano, Y., Ishimoto, H., Tokuno, M., Yoshizaki, Y., Okawara, N., 2002. Assessment of the nonsphericity of mineral dust from geostationary satellite measurements. Remote Sens. Environ. 82, 238–247.

Masuda, K., Mano, Y., Ishimoto, H., Tokuno, M., Yoshizaki, Y., Okawara, N., Yamagiwa, R., Uchiyama, A., Yamazaki, A., Tsutsumi, Y., 2003. Comparisons of the mineral dust optical thickness retrieved from geostationary satellite with ground based radiometer measurements. Remote Sens. Environ. 85, 484–488.

Masuda, K., Mano, Y., Ishimoto, H., Okawara, N., Yoshizaki, Y., 2005. Aerosol optical thickness over ocean derived from GMS-5 during Spring 2002 and 2003. J. Meteorol. Soc. Jpn. 83A, 173–186.

Matsuki, A., Iwasaka, Y., Osada, K., Matsunaga, K., Kido, M., Inomata, Y., Trochkine, D., Nishita, C., Nezuka, T., Sakai, T., 2003. Seasonal dependence of the long-range transport and vertical distribution of free tropospheric aerosols over east Asia: on the basis of aircraft and lidar measurements and isentropic trajectory analysis. J. Geophys. Res. 108 (D23).

Matsuki, A., Iwasaka, Y., Osada, K., Inomata, Y., Kim, Y-S., Trochkine, D., Nishita, C., Yamada, M., Nagatani, T., Shi, G., Chen, H., Zhang, D., Kido, M., Nagatani, M., Nakata, H., 2005. Observational insight Into the heterogeneous sulfate formation on dust surface: importance of the mineralogy and absorbed water. Proc. Fourth ADEC Workshop 325–328.

Mikami, M., Abe, O., Du, M., Chiba, O., Fujita, K., Hayashi, M., Iwasaka, Y., Kai, K., Masuda, K., Nagai, T., Oomoto, T., Suzuki, J., Uchiyama, A., Yabuki, S., Yamada, Y., Yasui, M., Shi, G., Zhang, X., Shen, Z., Wei, W., Zhou, J., 2002. The impact of aeolian dust on climate: Sino-Japanese cooperative project ADEC. J. Arid Land Stud. 11, 211–222.

Mikami, M., Yamada, Y., Ishizuka, M., Hayashi, M., Nagura, Y., Azuma, T., Zeng, F., Gao, W., 2004. An introduction of the wind erosion observation system for measuring dust emission process and its preliminary results at a Gobi Desert in the Taklimakan Desert, China. Proceedings of 1st general Assembly of European Geosciences Union.

Mikami, M., Yamada, Y., Ishizuka, M., Ishimaru, T., Gao, W., Zeng, F., 2005a. Measurement of saltation process over gobi and sand dunes in the Taklimakan desert, China, with newly developed sand particle counter. J. Geophys. Res. 110. doi:10.1029/2004JD004688 (D18S02).

Mikami, M., Aoki, T., Ishizuka, M., Yabuki, S., Yamada, Y., Gao, W., Zeng, F., 2005b. Observation of number concentration of desert aerosols in the south of the Taklimakan Desert, China. J. Meteorol. Soc. Jpn. 83A, 31–43.

Miller, R.L., Tegen, I., Perlwitz, J., 2004. Surface radiative forcing by soil dust aerosols and the hydrologic cycle. J. Geophys. Res. 109. doi:10.1029/2003JD004085 (D04203).

Motoyoshi, H., Aoki, Te., Hori, M., Abe, O., Mochizuki, S., 2005. Possible effect of anthropogenic aerosol deposition on snow albedo reduction at Shinjo, Japan. J. Meteorol. Soc. Jpn. 83A, 137–148.

Murayama, T., 2001. Formation of ice cloud from Asian dust particles in the upper troposphere. Proc. SPIE 4153, 218–225.

Murayama, T., Masonis, S.J., Redemann, J., Anderson, T.L., Schmid, B., Livingston, J.M., Russell, P.B., Huebert, B., Howell, S.G., McNaughton, C.S., Clarke, A., Abo, M., Shimizu, A., Sugimoto, N., Yabuki, M., Kuze, H., Fukagawa, S., Maxwell-Meier, K., Weber, R.J., Orsini, D.A., Blomquist, B., Bandy, A., Thornton, D., 2003. An intercomparison of lidar-derived aerosol optical properties with airborne measurements near Tokyo during ACE-Asia. J. Geophys. Res. 108 (D23), 8651. doi: 10.1029/2002JD003259.

Nakajima, T., Tonna, G., Rao, R., Kaufman, Y., 1996. Use of sky-brightness measurements from ground for remote sensing of particulate polydispersions. Appl. Opt. 35, 2672–2686.

Nakajima, T., Sekiguchi, M., Takemura, T., Uno, I., Higurashi, A., Kim, D., Sohn, B., Oh, J., Nakajima, S.N., Ohta, T.Y, Okada, S., Takamura, I., Kawamoto, T., 2003. Significance of direct and indirect radiative forcings of aerosols in the East China Sea region. J. Geophys. Res. 108 (D23), 8658. doi:10.1029/2002JD003261.

Nakawo, M., Fujita, K., 2005. Deposition history of dust particles and its impact on glaciers. Proceedings of Fourth ADEC, pp. 121–124.

Ohta, A., Kanai, Y., Terashima, S., Kamioka, H., Imai, N., Matsuhisa, Y., Shimizu, H., Takahashi, Y., Kai, K., Hayashi, M., Zhang, R., Tsumo, H., Kagi, H., Nomura, M., 2005. Elucidation of elemental behavior of aeolian dust transported from China to Japan. Proceedings of Fourth ADEC, pp. 297–300.

Owen, P.R., 1964. Saltation of uniform grains in air. J. Fluid Mech. 20, 225–242.

Sakai, T., Nagai, T., Nakazato, M., Matsumura, T., 2004. Raman lidar measurement of water vapor and ice clouds associated with Asian dust layer over Tsukuba, Japan. Geophys. Res. Lett. 31. doi:10.1029/2003GL019332 (L06128).

Sano, I., Mukai, S., Okada, Y., Holben, B.N., Ohta, S., Takamura, T., 2003. Optical properties of aerosols during APEX and ACE-Asia experiments. J. Geophys. Res. 108 (D23), 8649. doi:10.1029/2002JD003263.

Sassen, K., 2005. Dusty ice clouds over Alaska. Nature 434, 456.

Satake, S., Uno, I., Takemura, T., 2004. Numerical Study for the Radiative Impacts of Asian Tropospheric Aerosols. Engineering Science Reports, vol. 26. Kyusyu University, pp. 341–349 (in Japanese with English abstract).

Seino, N., Sasaki, H., Yamamoto, A., Mikami, M., Zhou, H., Zeng, F., 2005. Numerical simulation of mesoscale circulations in the Tarim Basin associated with dust events. J. Meteorol. Soc. Jpn. 83A, 205–218.

Shao, Y., 2000. Physics and Modeling of Wind Erosion. Atmospheric and Oceanographic Sciences Library, vol. 23. Kluwer Academic Press, Dordrecht, the Netherlands (393 pp.).

Shao, Y., 2005. A similarity theory for saltation and application to aeolian mass flux. Boundary-Layer Meteorol. 115, 319–338.

Shao, Y., Mikami, M., 2005. Heterogeneous saltation: theory, observation and comparison. Boundary-Layer Meteorol. 115, 359–379.

Shao, Y., Raupach, M.R., 1992. The overshoot and equilibration of saltation. J. Geophys. Res. 97 (D18), 20559–20564.

Shao, Y., Raupach, M.R., Leys, J.F., 1996. A model for predicting aeolian sand drift and dust entrainment on scales from paddock to region. Aust. J. Soil Res. 34, 309–342.

Shettle, E.P., Fenn, R.W., 1979. Models for the Aerosols of the Lower Atmosphere and the Effects of Humidity Variations on their Optical Properties. Air Force Geophysics Laboratory. AFGL-TR-79-0214, (94 pp.).

Shi, G.-Y., 1998. On the k-Distribution and Correlated k-distribution Models in the Atmospheric Radiation Calculations. Scientia Atmospherica Sinica (Special Issue Dedicated to the 70th Anniversary of the Founding of the Institute of Atmospheric Physics, Chinese Academy of Sciences) 22, 555–576.

Shi, G-Y., Wang, H., Wang, B., Li, W., Gong, S., Zhao, T., Aoki, T., 2005. Sensitivity experiments on the effects of optical properties of dust aerosols on their radiative forcing under clear sky condition. J. Meteorol. Soc. Jpn. 83A, 333–346.

Sokolik, I., Golitsyn, G., 1993. Investigation of optical and radiative properties of atmospheric dust aerosols. Atmos. Environ. 27A, 2509–2517.

Sokolik, I., Winker, D.M., Bergametti, G., Gillette, D.A., Carmichael, G., Kaufman, Y., Gomes, L., Schuetz, L., Penner, J.E., 2001. Introduction to special section: outstanding problems in quantifying the radiative impacts of mineral dust. J. Geophys. Res. 106, 18,015–18,028.

Takemi, T., 2005. Explicit simulations of convective-scale transport of mineral dust in severe convective weather. J. Meteorol. Soc. Jpn. 83A, 187–203.

Takemi, T., Yasui, M., Zhou, J., Liu, L., 2005. Modeling study of diurnally varying convective boundary layer and dust transport over desert regions. SOLA 1, 157–160. doi:10.2151/sola.2005-041.

Takemura, T., Okamoto, H., Murayama, Y., Numaguti, A., Higurashi, A., Nakajima, T., 2000. Global three-dimensional simulation of aerosol optical thickness distribution of various origins. J. Geophys. Res. 105, 17853–17873.

Takemura, T., Nakajima, T., Dubovik, O., Holben, B.N., Kinne, S., 2002. Single-scattering albedo and radiative forcing of various aerosol species with a global three-dimensional model. J. Climate 15, 15333–15352.

Takemura, T., Nakajima, T., Higurashi, A., Ohta, S., Sugimoto, N., 2003. Aerosol distributions and radiative forcing over the Asian Pacific region simulated by Spectral Radiation–Transport Model for Aerosol Species (SPRINTARS). J. Geophys. Res. 108. doi:10.1029/2002JD003210.

Tanaka, T.Y., Chiba, M., 2005. Global simulation of dust aerosol with a chemical transport model, MASINGAR. J. Meteorol. Soc. Jpn. 83A, 255–278.

Tanaka, T.Y., Orito, K., Sekiyama, T.T., Shibata, K., Chiba, M., Tanaka, H., 2003. MASINGAR, a global tropospheric aerosol chemical transport model coupled with MRI/JMA98 GCM: model description. Pap. Meteorol. Geophys. 53, 119–138.

Tanaka, T.Y., Kurosaki, Y., Chiba, M., Matsumura, T., Nagai, T., Yamazaki, A., Uchiyama, A., Tsunematsu, N., Kai, K., 2005. Possible transcontinental dust transport from north Africa and the middle east to east Asia. Atmos. Environ. 39, 3901–3909.

Tegen, I., Harrison, S.P., Kohfeld, K., Prentice, I.C., Coe, M., Heimann, M., 2002. Impact of vegetation and preferential source areas on global dust aerosol: results from a model study. J. Geophys. Res. 107 (D21), 4576. doi:10.1029/2001JD000963.

Tsunematsu, N., Kai, K., Matsumoto, T., in press. The influence of synoptic-scale air flow and local circulation on the dust layer height in the north of the Taklimakan Desert. Water, Air, Soil Pollution.

Tsor, H., Pye, K., 1987. Dust transport and the question of desert loess formation. Sedimentology 34, 139–153.

Uchiyama, A., Yamazaki, A., Togawa, H., Asano, J., 2005a. Absorption property of aeolian dust as inferred from sky-radiometer and ground-based measurement. Proceedings of the Fourth ADEC Workshop.

Uchiyama, A., Yamazaki, A., Togawa, H., Asano, J., 2005b. Characteristics of aeolian dust observed by sky-radiometer in the ADEC Intensive Observation Period 1(IOP1). J. Meteorol. Soc. Jpn. 83A, 291–305.

Uno, I., Amano, H., Emori, S., Kinoshita, K., Matsui, I., Sugimoto, N., 2001. Trans-Pacific Yellow Sand Transport observed in April 1998: numerical simulation. J. Geophys. Res. 106, 18331–18344.

Uno, I., Satake, S., Carmichael, G.R., Tang, Y., Wang, Z., Takemura, T., Sugimoto, N., Shimizu, A., Murayama, T., Cahill, T.A., Cliff, S., Uematsu, M., Ohta, S., Quinn, P., Bates, K., 2004. Numerical study of Asian dust transport during the springtime of 2001 simulated with the Chemical Weather Forecasting System (CFORS) model. J. Geophys. Res. 109. doi:10.1029/2003JD004222 (D19S24).

Uno, I., Harada, K., Satake, S., Hara, Y., Wang, Z., 2005a. Meteorological characteristics and dust distribution of the Tarim Basin simulated by the nesting RAMS/CFORS dust model. J. Met. Soc. Japan. 83A, 219–239. 18(D16), 155-18, 166.

Uno, I., Wang, Z., Chiba, M., Chun, Y.S., Gong, S.L., Hara, Y., Jung, E., Lee, S.S., Liu, M., Mikami, M., Music, S., Nickovic, S., Satake, S., Shao, Y., Song, Z., Sugimoto, N., Tanaka, T., Westphal, D.L., in press. Dust model intercomparison (DMIP) study over Asia — Overview. J. Geophys. Res.

Wang, Z., Ueda, H., Huang, M., 2000. A deflation module for use in modeling long-range transport of yellow sand over east Asia. J. Geophys. Res. 105, 26,947–26,957.

Werner, M., Tegen, I., Harrison, S.P., Kohfeld, K.E., Prentice, I.C., Balkanski, Y., Rodhe, H., Roelandt, C., 2002. Seasonal and interannual variability of the mineral dust cycle under present and glacial climate conditions. J. Geophys. Res. 107 (D24), 4744. doi:10.1029/ 2002JD002365.

Woodward, S., 2001. Modeling the atmospheric life cycle and radiative impact of mineral dust in the Hadley Center climate model. J. Geophys. Res. 106, 18155–18166.

World Meteorological Organization (WMO), 1974. Manual on Codes, Vol. I, International Codes, WMO Publ., 306, WMO, Geneva.

Xie, F., Wang, J., Uno, I., 2005. How about the difference of dust emission in simulating severe dust storms in the DMIP? Proceedings of Fourth ADEC, pp. 91–94.

Yabuki, S., Kanayama, S., Fu, F., Honda, M., Yanagisawa, F., Wei, W., Zeng, F., Liu, M., Shen, Z., Liu, L., 2002. Physical and chemical characteristics of aeolian dust collected over Asian dust source regions in China — comparison with atmospheric aerosols in an urban area at Wako, Japan. J. Arid Land Stud. 11, 273–289.

Yabuki, S., Kanayama, S., Yanagisawa, F., Nagamura, Y., Matsumomto, H., Zhou, H., Liu, M., Zeng, F., Liu, L., Shen, Z., 2005a. Summery of three-years-observation of aerosols at four observation sites over Asian dust source areas. Proceedings of the Fourth ADEC, pp. 15–18.

Yabuki, S., Mikami, M., Nakamura, Y., Kanayama, S., Fu, F., Liu, M., Zhou, H., 2005b. Aerosol characteristics at Aksu in the Asian dust source region of north-west China — summary of the three years' observation from March 2001 to April 2004. J. Meteorol. Soc. Jpn. 83A, 45–72.

Yamada, Y., Mikami, M., Nagashima, H., 2002. Dust particle sampling system for streamwise dust flux. J. Arid Land Stud. 11-4, 229–234.

Yamashita, K., Hayashi, M., Irie, M., Yamamoto, K., Saga, K., Ashida, M., Shiraishi, K., Okabe, K., 2005. Amount and state of mineral particles in the upper mixed layer and the lower free troposphere over Mt. Raizan, southwestern Japan: unmanned airplane measurements in the Spring of 2003. J. Meteorol. Soc. Jpn. 83A, 121–136.

Yasui, M., Zhou, J., Liu, L., Itabe, T., Mizutani, K., Aoki, T., 2002. Lidar measurements of the airborne dust in Shapatou: preliminary results in the Springtime 2001. J. Arid Land Stud. 11, 315–320.

Yasui, M., Kai, K., Iwasaka, Y., Shibata, T., Nagai, T., Chiba, M., Fujiwara, M., Shiraishi, K., Zhou, J., Liu, L., Shen, Z., Zhou, H., Shi, G., 2005a. Dust profile observed by ADEC Lidar Network. Proceedings of Fourth ADEC Workshop, pp. 29–32.

Yasui, M., Zhou, J., Liu, L., Itabe, T., Mizutani, K., Aoki, T., 2005b. Vertical profiles of aeolian dust in a desert atmosphere observed using lidar in Shapatou, China. J. Meteorol. Soc. Jpn. 83A, 149–171.

Yoshino, M., 2002. Secular variations of sand–dust storm and blown sand occurrence in the Taklimakan Desert, NW China. J. Arid Land Stud. 11, 253–258.

Zender, C.S., Bian, H., Newman, D., 2003. Mineral Dust Entrainment and Deposition (DEAD) model: description and 1990s dust climatology. J. Geophys. Res. 108 (D14), 4416. doi:10.1029/2002JD002775.

Zhang, D., Iwasaka, Y., 2004. Size change of Asian dust particles caused by sea salt interaction: measurements in southwestern Japan. Geophys. Res. Lett. 31. doi:10.1029/2004GL020087.

Zhang, D., Iwasaka, Y., 2005. Mixing of Asian dust particles and sea salt and its potential importance. Proceedings of Fourth ADEC, pp. 345–348.

Zhao, C., Dabu, X., Li, Y., 2004. Relationship between climatic factors and dust storm frequency in Inner Mongolia of China. Geophys. Res. Lett. 31. doi:10.1029/2003GL018351.